

Salt adaptation requires efficient fine-tuning of jasmonate signalling

Ahmed Ismail · Mitsunori Seo · Yumiko Takebayashi · Yuji Kamiya · Elisabeth Eiche · Peter Nick

Received: 4 October 2013 / Accepted: 20 November 2013 / Published online: 3 December 2013
© Springer-Verlag Wien 2013

Abstract Understanding the mechanism by which plants sense, signal and respond to salinity stress is of great interest to plant biologists. In stress signalling, often the same molecules are involved in both damage-related and adaptive events. To dissect this complexity, we compared the salinity responses of two grapevine cell lines differing in their salinity tolerance. We followed rapid changes in the cellular content of sodium and calcium, apoplastic alkalisation and slower responses in the levels of jasmonic acid, its active isoleucine conjugate and abscisic acid, as well as of stilbenes. Differences in timing and sensitivity to either the lanthanoid Gd or exogenous calcium provide evidence for an adaptive role of early sodium uptake through non-selective cation channels acting upstream of Ca^{2+} and H^+ fluxes. We find a

correlation of salt sensitivity with unconstrained jasmonate (JA) signalling, whereas salt adaptation correlates with tight control of jasmonic acid and its isoleucine conjugate, accompanied by accumulation of abscisic acid and suppression of stilbenes that trigger defence-related cell death. The data are discussed by a model where efficient fine-tuning of JA signalling determines whether cells will progress towards adaptation or programme cell death.

Keywords Salinity stress · Grapevine (*V. rupestris*, *V. riparia*) · JAs · ABA · JAZ proteins · Cytosolic Ca^{2+} · Apoplastic pH · Suppression machinery · Stilbene compounds · PCD · NSCCs

Handling Editor: Bhumi Nath Tripathi

Electronic supplementary material The online version of this article (doi:10.1007/s00709-013-0591-y) contains supplementary material, which is available to authorized users.

A. Ismail · P. Nick
Molecular Cell Biology, Botanical Institute, Karlsruhe Institute of Technology (KIT), Karlsruhe, Germany

A. Ismail (✉)
Department of Horticulture, Faculty of Agriculture, Damanhour University, El-Goumhoriya St. 42, 22516 Damanhour, Egypt
e-mail: ahmed.ismail@damanhour.edu.eg

M. Seo · Y. Takebayashi
RIKEN Plant Science Center, Tsurumi, Yokohama, Kanagawa 230-0045, Japan

Y. Kamiya
RIKEN Center for Sustainable Resource Science, Yokohama, Kanagawa 230-0045, Japan

E. Eiche
Institut of Mineralogy und Geochemistry, Karlsruhe Institute of Technology (KIT), Karlsruhe, Germany

Introduction

Life requires that an internal homeostasis is continuously defended against fluctuations of the environment. When this homeostasis is lost in consequence of external challenges, the organism experiences stress. Stress conditions will induce adaptive responses aimed to re-establish homeostasis. Since plants cannot run away, stress adaptation is their only remedy to cope with the adversities of life. The signals culminating in stress adaptation have therefore been of central scientific interest and great agronomical impact (for reviews, see Ingram and Bartels 1996; Hasegawa et al. 2000; Zhu 2002; Huang et al. 2012). A very simple mechanism to respond appropriately to stress would be to use stress-induced imbalance or its cellular consequences (in the following designated by the term *stress damage*) as signal to activate *stress adaptation*. In fact, this is the case for reactive oxygen species (ROS) that play a dual role as toxic by-products of stress-evoked metabolic imbalance and as central signals for the adaptation to osmotic stress (for review, see Miller et al. 2010). It is therefore far from trivial to discriminate events linked with *stress damage* from the events that confer *stress adaptation*. To assign a given event to either *stress*

damage or *stress adaptation*, it is necessary to define timing as well as the phenotype observed upon inactivation or activation of this event.

Salt stress is considered to be a major constraint for many crop plants and has been a threat to agriculture in some parts of the world for more than 3,000 years (Flowers, 2006). More than 80 million ha of arable land worldwide is estimated to be affected by salt (Munns and Tester 2008) resulting in estimated annual global costs equivalent to US \$11,000 million in 2011 (FAO 2011; <http://www.fao.org/ag/agl/agll/spush/>). Sodium ions from the soil enter the cortical cytoplasm of plant roots by passive transport (Tester and Davenport 2003) via non-selective cation channels (NSCCs) that have been classified according to their voltage dependence or to their responsiveness to certain ligands and physical stimuli (Demidchik and Maathuis 2007; Essah et al. 2003; Kronzucker and Britto 2011).

Salinity-dependent stress damage includes loss of turgescence (leading to growth arrest), membrane disorganisation, metabolic imbalance, formation of ROS, inhibition of photosynthesis and reduced nutrient acquisition (for reviews, see Hasegawa et al. 2000; Zhu 2002). The cellular response depends also on the timing: It differs for a situation, where salt concentration is increased instantaneously from a situation, where the concentration increases slowly over a longer period (which is the natural situation). This distinction has been termed “salt shock” versus “salt stress” (Shavrukov 2013) and adds a further level of complexity. However, as in most experiments, in the current study we used the design of a “salt shock” to get a clearer temporal sequence of responses. To achieve stress adaptation, the cell has to: (1) restore turgescence (the swelling process) against the inverted gradient of water potential (Felix et al. 2000; Zimmermann et al. 2008) and (2) quell damage-related signalling to escape programmed cell death (PCD) (Hasegawa et al. 2000). The velocity and amplitude of these adaptive responses will define the degree of salinity tolerance of the respective plant. To restore turgescence is necessary in order to recover growth. Since the gradient of water potential is inverted upon salinity stress, the protoplast has to build up osmotic potential, while maintaining ionic homeostasis in the cytoplasm. This can be achieved by production of compatible osmolytes such as betaine or proline (Hasegawa et al. 2000; Yoshihara et al. 1995), by absorption of ions in the apoplast through electrostatic interaction with the cell wall or by accumulating ions in the vacuole. The vacuolar Na⁺/H⁺ exchanger 1 (NHX1), in concert with other members of this family of transporters, plays a crucial role in this context because it will repartition Na⁺ ions into the vacuole. In fact, NHX1 has been successfully employed to improve osmotic tolerance upon overexpression (Apse et al. 1999; Gaxiola et al. 1999).

On the other side, Na⁺ ions penetrating into the cytoplasm, for instance through the NSCCs, have to be extruded. This is

achieved through the salt overly sensitive 1 (SOS1) Na⁺/H⁺ antiporter in the plasma membrane. The deformation of the membrane due to the reduced turgescence activates Ca²⁺ influx channels in the plasma membrane (Knight et al. 1997) and (probably through stimulation of phospholipase D, Hong et al. 2008) generates IP₃ as secondary messenger that will transduce the signal to the tonoplast and triggers IP₃-dependent Ca²⁺ channels there. The resulting rise in cytoplasmic Ca²⁺ is sensed by the Ca²⁺-binding SOS3 protein that activates the kinase SOS2, which subsequently phosphorylates the SOS1. The activated SOS1 extrudes Na⁺ from the cell, such that metabolism is protected against ionic imbalance (Harper et al. 2004; Munns and Tester 2008; Zhu 2002). The plasma membrane-targeted SOS and the tonoplast-located NHX systems are interconnected by activation of NHX1 by the SOS2 kinase (Qiu et al. 2004).

In addition to restoring osmotic gradients and ionic balance, adaptation to salt stress requires that ROS homeostasis is restored. This is achieved by different ROS-scavenging machineries that tightly control the ROS levels both enzymatically and non-enzymatically (Apel and Hirt 2004). In this context, stilbenes, better known as antifungal phytoalexins, act as ROS scavengers (Derckel et al. 1999; Petit et al. 2009). The most prominent stilbene is resveratrol (3,5,4'-trihydroxystilbene), which for its ROS-scavenging activity has attracted considerable medical interest, since it is effective as antioxidant, antimutagen and anti-inflammatory agent and even prevents the progression of human promyelocytic leukaemia (Jang et al. 1997; Wang et al. 2010). However, in plant cells, resveratrol acts as signal triggering PCD which makes sense in the context of a pathogen attack (Chang et al. 2011), but not in the context of salt stress. This implies that efficient salt adaptation must circumvent or quell the induction of defence-related responses that participate in PCD.

In addition to ion channels and ROS scavengers, the phytohormones ABA and jasmonates (JAs) play a central role in plant adaptation to stress conditions. The role of ABA for osmotic adaptation has long been recognized and intensively studied. For example, ABA increases salinity tolerance by activating stress-responsive genes that encode enzymes for the biosynthesis of osmolytes (e.g. betaine), or protective proteins, such as dehydrins, and LEA-like proteins (Gao et al. 2004; Hasegawa et al. 2000). However, for other hormones that accumulate in response of salinity, it is not clear whether their increase is adaptive or simply a manifestation of *stress damage*: JAs, for instance, have been shown to be induced by osmotic stress (Creelman and Mullet 1995; Lehmann et al. 1995), and a correlation between salt tolerance and the steady-state levels of JA has been drawn for two tomato cultivars (Pedranzani et al. 2003). However, when this JA induction was investigated in a more quantitative manner in salt-stressed rice roots, JA was found to be induced much later and only modestly as compared to ABA. Only for very

high concentrations of salt close to lethality the induction of JA became dominant (Moons et al. 1997). Moreover, JA antagonized ABA with respect to the induction of adaptive genes. In our previous work, we have analysed the role of JA for the induction of an osmoprotective PR10 protein (RSOsPR10) in the same system, rice roots (Takeuchi et al. 2011), and we could show that the RSOsPR10 transcript is also activated, in a manner similar to the wild type, in a rice mutant that cannot synthesize any JA. Thus, although strong activation of the JA pathway is accepted as key event of plant defence (Browse 2009) required to induce typical defence proteins, such as proteinase inhibitors or enzymes involved in phytoalexin synthesis (Wasternack 2007), adaptive responses to salt stress seem to be accompanied by a more constrained induction of the JA pathway. In fact, there exists a multimeric transcriptional corepression complex machinery to suppress JA signalling: In *Arabidopsis thaliana*, 12 JAZ/TIFY proteins, the corepressor TOPLESS (TPL), TPL-related proteins (TPRs) and a novel interactor of JAZ (NINJA) participate in this machinery (Chini et al. 2007; Thines et al. 2007; Pauwels et al. 2010) indicating that JA signalling must be tightly controlled to avoid hazardous side effects. This complexity is further amplified by ramifications of the pathway into several bioactive derivatives of JA: Conjugation with isoleucine by the jasmonate-resistant 1 enzyme generates (+)-7-iso-jasmonoyl-*l*-isoleucine (JA-II) as endogenous JA species with the highest bioactivity (Staswick and Tiryaki 2004; Staswick 2008; Fonseca et al. 2009). The role of JA-II, to our knowledge, so far has not been investigated in the context of salinity stress.

This short overview, which is far from complete, may suffice to demonstrate that adaptation to salinity is not provided by one single “master-switch” but must have evolved from tuning the cross-talk of different regulatory circuits. To address these circuits, we decided to make use of natural biodiversity in a system, where osmotic adaptation can be studied in contrast to defence-related signalling. We employed two cell lines from two closely related grapevine species differing in osmotic tolerance (Ismail et al. 2012): *Vitis rupestris* inhabits rocky, sunny slopes and therefore has evolved a considerable osmotic tolerance. In contrast, *Vitis riparia* occurs in alluvial woods and performs poorly under osmotic stress. During previous studies, we could show that different genotypes of grapevine cell lines accumulate different levels and types of ROS-scavenging stilbenes in a defence context (Chang et al. 2011), and we have mapped these differences with respect to defence-related signalling (Chang and Nick 2012). In addition to these experimental prerequisites, *Vitis* was chosen for its agronomical relevance. Grapevine is the economically most important fruit species worldwide, and since it is preferentially cultivated in semiarid regions, osmotic tolerance is a central issue. In a previous study (Ismail et al. 2012), we could show that in the osmotic-tolerant *V. rupestris*, cell line members of the JAZ/TIFY family were more rapidly

and more strongly induced indicating that there exists a correlation between osmotolerance and the suppression of JA signalling. In the current work, we test and confirm the hypothesis that, in the context of salinity stress, unconstrained JA signalling classifies as damage-related event that has to be controlled to acquire adaptation to salinity.

Materials and methods

Cell lines and treatments

Suspension cell cultures of *V. rupestris* and *V. riparia* generated from leaves (Seibicke 2002) (see supplemental Fig. 1) were cultivated in liquid medium containing 4.3 g l⁻¹ Murashige–Skoog salts (Duchefa, Haarlem, the Netherlands), 30 g l⁻¹ sucrose, 200 mg l⁻¹ KH₂PO₄, 100 mg l⁻¹ inositol, 1 mg l⁻¹ thiamine and 0.2 mg l⁻¹ 2,4-dichlorophenoxyacetic acid, pH 5.8. The microelements of the Murashige–Skoog medium are composed of 0.025 mg l⁻¹ CoCl₂·6H₂O, 0.025 mg l⁻¹ CuSO₄·5H₂O, 36.70 mg l⁻¹ FeNaEDTA, 6.20 mg l⁻¹ H₃BO₃, 0.83 mg l⁻¹ KI, 16.90 mg l⁻¹ MnSO₄·H₂O, 0.25 mg l⁻¹ NaMoO₄·2H₂O and 8.60 mg l⁻¹ ZnSO₄·7H₂O, while the macroelements are 332.02 mg l⁻¹ CaCl₂, 170.00 mg l⁻¹ KH₂PO₄, 1,900.00 mg l⁻¹ KNO₃, 180.54 mg l⁻¹ MgSO₄ and 1,650.00 mg l⁻¹ NH₄NO₃. Cells were subcultured weekly; 10 ml of stationary cells was inoculated into 30 ml of fresh medium in 100 ml Erlenmeyer flasks. The cell suspensions were incubated at 25 °C in the dark on an orbital shaker (KS250 basic, IKA Labor Technik, Staufen, Germany) at 150 rpm.

To induce cellular responses, cultures were treated at day 5 after subcultivation with 155 mM NaCl, 1 mM CaCl₂ or water as a negative control. In some experiments, a bona fide inhibitor of both Ca²⁺ influx (Knight et al. 1997) and NSCCs (Demidchik et al. 2002) gadolinium chloride (GdCl₃) at 0.75 mM (Sigma-Aldrich, Deisenhofen, Germany) was added 2 min before administering salinity stress.

Measurement of PCV, extracellular pH and mortality as responses to salt stress

Packed cell volume (PCV) as a measure of growth was recorded in response to different concentrations of NaCl (50, 85, 155 mM). The relative increment in PCV, $(\Delta V_t/V_t)/(\Delta t)$, was used as measure of the growth response. Each data point represents mean and standard error of at least three independent experimental series, collected daily after subcultivation over 8 days.

Apoplasmic alkalisation was followed by a pH meter (Schott handylab, pH 12) connected to a pH electrode (Mettler Toledo, LoT403-M8-S7/120) and recorded by a paperless recorder (VR06; MF Instruments GmbH, Albstadt-Truchtelfingen, Germany) at 1-s intervals. Before induction,

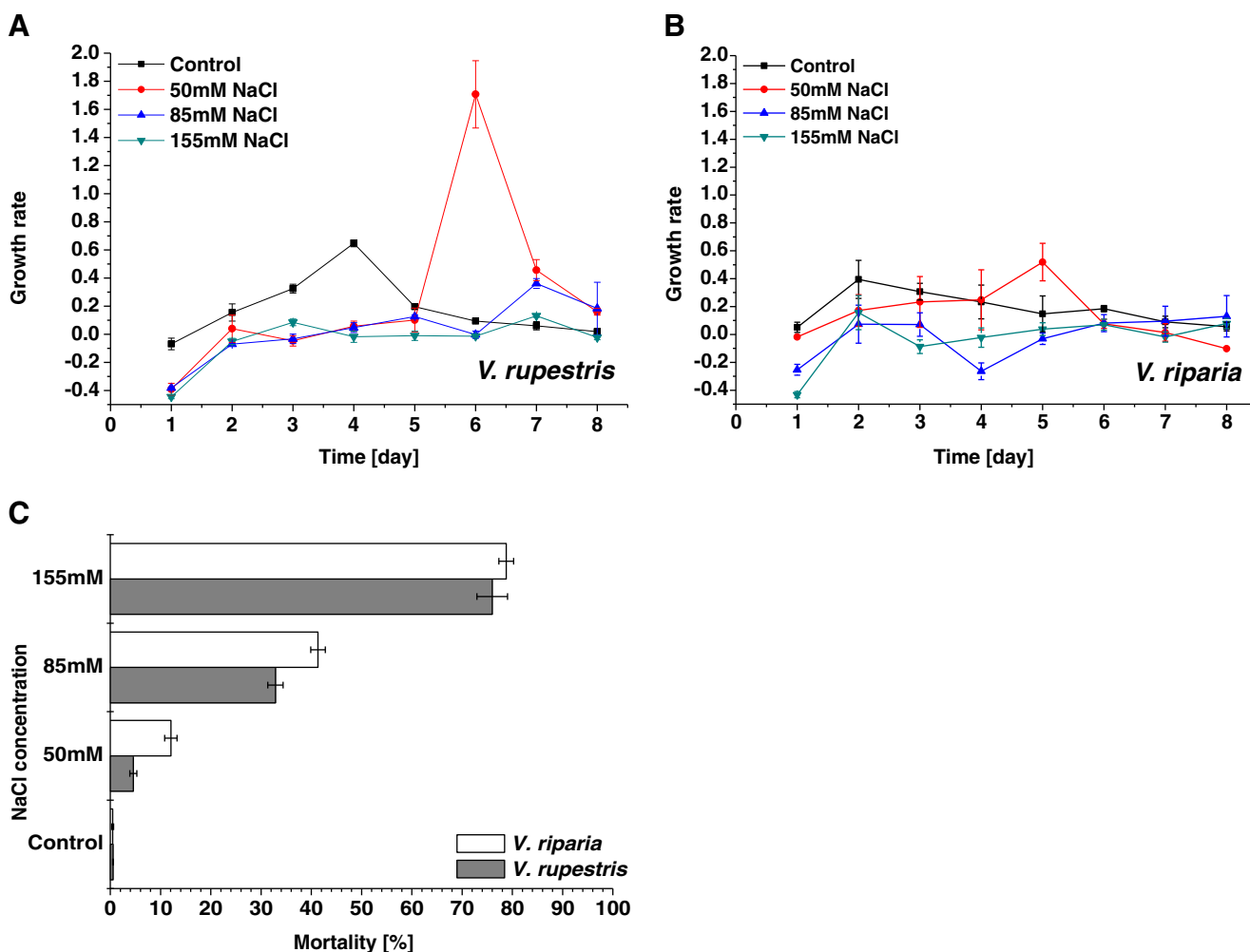


Fig. 1 Time course of relative growth rate ($\Delta V_t/V_t$ over Δt) during salt stress in *V. rupestris* (a) versus *V. riparia* (b) for different concentrations of NaCl. c Mortality (in percent) at day 8 for the two genotypes. Data represent mean values and standard errors from three independent experimental series

2 ml of suspension cells (4 days after subcultivation) was pre-adapted on an orbital shaker (~90 rpm) for ~90 min, until the pH was stable (pH~5). To test the effect of salt on extracellular pH, cells were treated with 155 mM NaCl for 30 min. To block the induction of apoplastic pH, cells were pretreated with different concentrations of GdCl₃ or water for 2 min before the addition of salt. The pH data were exported to Microsoft Office Excel by the data acquisition software Observer II_V2.35 (MF Instruments GmbH). Mortality was assessed according to the method by Gaff and Okong'O-Ogola (1971) using 2.5 % (w/v) Evans Blue (Sigma-Aldrich, Neu-Ulm, Germany) in aliquots of 200 μ l using custom-made staining chambers to remove the medium.

Measurement of cellular Na⁺ and Ca²⁺ content

Cells were treated with 155 mM NaCl at day 5 after subcultivation and incubated on a shaker for 2, 5, 10, 15, 30 min, 1, 2, 3 and 6 h at 150 rpm. At each time point, the

medium components were three times washed off with isotonic mannitol solution using a Büchner funnel under vacuum (Babourina et al. 2000) and then dried at 80 °C overnight. After determining dry weight, cells were digested according to Ippolito and Barbarick (2000) with minor modifications as follows: Dry cells of each biological replicate were transferred into digestion tubes (Gerhardt, UK), supplemented with 5 ml of concentrated nitric acid (HNO₃) and then incubated for at least 24 h at room temperature while vortexing at 6 and 24 h. Samples were placed on a water bath at 100 °C for 2 h. After cooling, the final volume of each sample was adjusted to 10 ml with distilled water and vortexed. Na⁺ and Ca²⁺ contents were measured by flame atomic absorption spectrometry (AAAnalyst200, Perkin Elmer) in an air-acetylene flame (Institute of Mineralogy and Geochemistry, Karlsruhe Institute of Technology). Blank samples were prepared by adding 5 ml concentrated nitric acid on an empty digestion vessel and processed as described above. Additionally, 155 mM NaCl was applied to the cells after pretreatment with 0.75 mM GdCl₃ for 2 min followed by the

same procedure. In a third set of experiments, 1 mM CaCl₂ was added alone or directly prior to salt. Concentrations were calculated with reference to dry weight from three independent biological replicates.

Quantification of phytohormones

Phytohormone contents were quantified for both cell lines with three biological replicates at 1, 3 and 6 h after addition of 155 mM NaCl alone or preceded by pretreatment with 0.75 mM GdCl₃ (0.75 mM) for 2 min. As controls, cells were treated in the same manner for 1 h with water or with 0.75 mM GdCl₃. Additionally, 1 mM CaCl₂ was applied in the absence of salt for either 1 or 3 h. All samples were collected by removing the supernatant using a Büchner funnel under vacuum. Both cells and supernatants were shock-frozen in liquid nitrogen, freeze-dried at -50 °C for 2 days and weighed. Plant hormones were extracted as described previously (Yoshimoto et al. 2009) with some modifications: Lyophilized cultured cells or culture media were homogenized in 4 ml of 80 % acetonitrile (MeCN) containing 1 % acetic acid and extracted for 30 min with internal standards (¹³C₆-JA-II, d₂-JA, d₆-SA, d₆-ABA and d₂-IAA). After centrifugation at 1,663×g for 20 min, the supernatant was collected and the sediment extracted again with 4 ml of 80 % MeCN containing 1 % acetic acid. One millilitre (for cultured cells) or 4 ml (for culture media) of the supernatant was processed further for hormone analysis. After removing MeCN in the supernatant, the acidic aqueous extract was loaded onto an Oasis HLB column cartridge (30 mg, 1 ml Waters, Milford, MA, USA) and washed with 1 ml of water containing 1 % acetic acid to remove highly polar impurities. Plant hormones were eluted with 2 ml of 80 % MeCN containing 1 % acetic acid. Ten percent of the eluate was used for the analysis of salicylic acid (SA). After removing MeCN in the remaining eluate, the acidic water extract was loaded onto an Oasis WAX column cartridge (30 mg, 1 ml). After washing with 1 ml of water containing 1 % acetic acid, neutral compounds were removed with 2 ml of 80 % MeCN, and acidic compounds were eluted with 2 ml of 80 % MeCN containing 1 % acetic acid. Hormones were quantified by liquid chromatography–electrospray ionisation–tandem mass spectrometry as described in detail in Yoshimoto et al. (2009). For salt-induced hormones in supernatant samples, see supplemental Fig. 2.

Extraction and quantification of stilbenes

The production of stilbenes as ROS scavengers was tested for both cell lines after challenge with 155 mM NaCl at different time points (0, 2, 4, 6, 8, 10, 24 or

48 h). The treated cells were harvested by centrifugation (5,000 rpm, 5 min) to remove media, weighed, directly frozen in liquid nitrogen and then stored at -80 °C until analysis. Stilbenes were extracted according to Tassoni et al. (2005) with minor modifications. Twenty millilitres of 80 % (v/v) methanol in water was added to 3–5 g fresh weight. The mixture was then homogenized by an ultrasonic processor (UP100H, Hielscher, Germany) for 3 min. The homogenate was shaken for 2 h in the dark at room temperature and filtered through filter paper under vacuum with 500 pa. The filtrate was concentrated to a residual volume of 5 ml in a glass tube at 40 °C (Heating Bath B490, BÜCHI, Essen, Germany) at 280 rpm (Rotavapor R-205, BÜCHI, Essen, Germany), under a vacuum of 80 Pa (Vacuubrand CVC2, Brand, Germany). Water-soluble stilbenes were extracted by adding 2 ml of 5 % (w/v) NaHCO₃ and three aliquots of 5 ml ethyl acetate. The pooled ethyl-acetate phase was completely dried to yield a stilbenic residue on the bottom of the glass tube. The residue was resuspended in 2 ml of methanol for analysis by high-performance liquid chromatography (HPLC).

Stilbenes were analysed by HPLC (Agilent, 1200 series, Waldbronn, Germany) using a Phenomenex Synergi hydro RP column (150×4.6 mm, particle size 4 µm, Phenomenex; Aschaffenburg, Germany), a DAD detector and a quaternary valve. The flow rate was adjusted to 0.8 ml min⁻¹, and the injection volume was 20 µl. The UV–Vis spectra were recorded from 200 to 400 nm. The mobile phases included acetonitrile (ACN), methanol and water in the following isocratic gradient: 2 min ACN/water (10:90 v/v), 15 min ACN/water (40:60 v/v), 30 min ACN/methanol (50:50 v/v), 32 min ACN/methanol (5:95 v/v), 35 min ACN/methanol (5:95 v/v), 39 min ACN/water (10:90 v/v) and 42 min ACN/water (10:90 v/v). *Trans*-resveratrol, *trans*-piceid and δ-viniferin were quantified and identified using an external standard on the basis of retention time and UV–Vis spectra. The standards for *trans*-resveratrol (Sigma-Aldrich, Deisenhofen, Germany), *trans*-piceid (Phytolab, Vestenbergsgreuth, Germany) and δ-viniferin (kind gift of Dr. Kassemeyer, State Institute of Viticulture, Freiburg, Germany) were dissolved in methanol to a concentration of 100 mg l⁻¹. Calibration curves determined using these standards were linear ($r^2 > 0.99$) and used for quantification of the samples (Chang et al. 2011). At least four biological replicates were analysed for each time point.

Statistical analysis

The treatments of the current study were arranged as a factorial experiment in a completely randomized

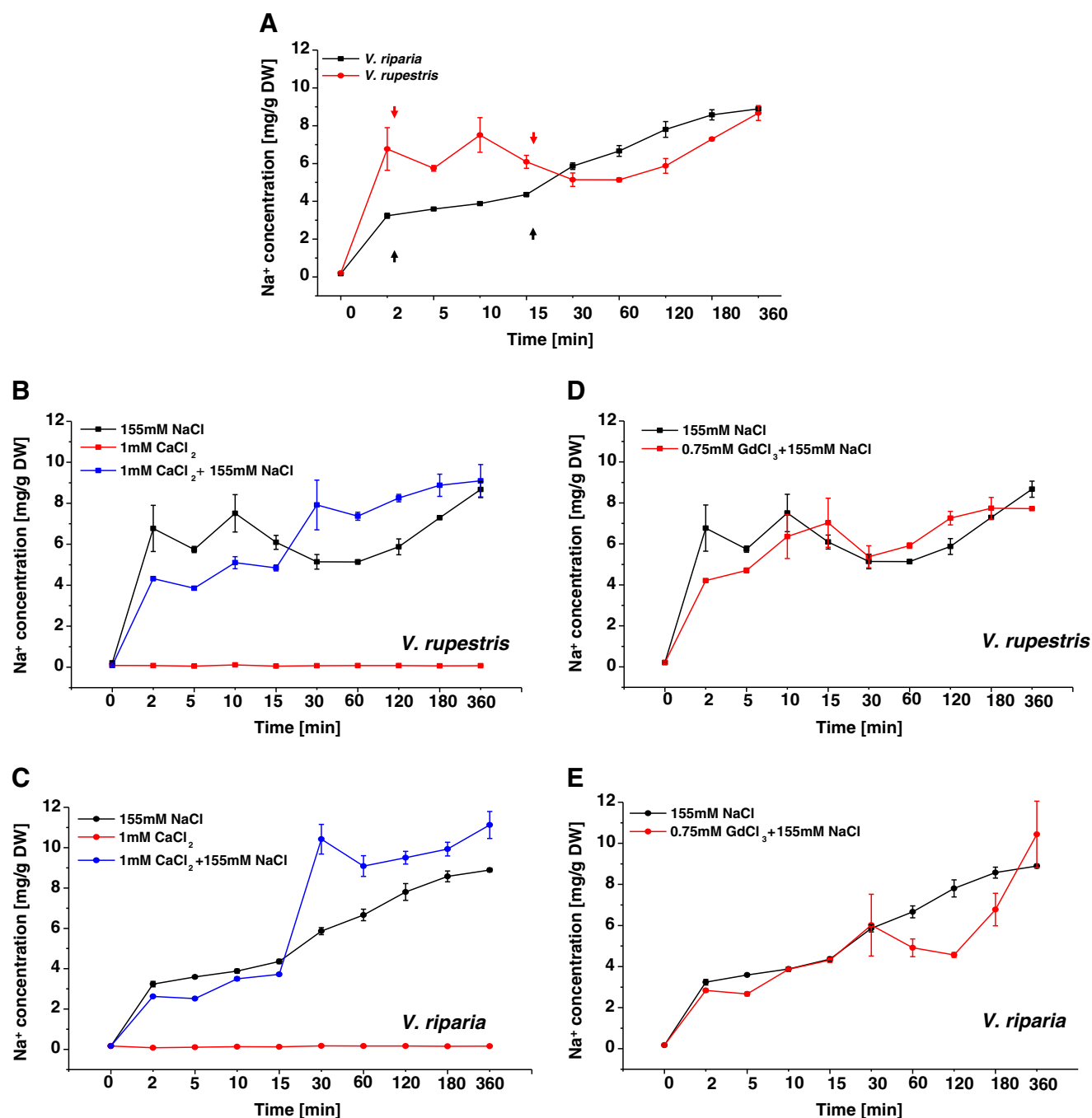


Fig. 2 Time course of Na⁺ uptake upon continuous challenge with 155 mM NaCl in control cells (**a**) of *V. rupestris* (red) versus *V. riparia* (black) and after pretreatment with 1 mM CaCl₂ (**b**, **c**) or 750 μM GdCl₃ (**d**, **e**) for *V. rupestris* (**b**, **d**) and *V. riparia* (**c**, **e**). Data represent mean values and standard errors from three independent experimental series. As

negative control in **b** and **c**, Na⁺ content after pretreatment of Ca²⁺ without subsequent salinity exposure was recorded (red lines). The arrows in **a** indicate begin and end of the phase II defined in the text. To resolve the early time points, the time axis is plotted in a non-linear scale

design. Three biological replicates were analysed for each treatment. Comparisons among means were made via the least significant differences (LSD) ($P < 0.05$) multiple ranges by using the SAS (2000) software. Mean values and standard error of the mean were calculated using Microsoft Excel.

Results

Growth resumes under salinity in *V. rupestris* and in *V. riparia*

As experimental system for the present study, we employed two grapevine cell lines from genotypes that differ in their

sensitivity to drought. The wild North American grape *V. rupestris*, used in viticulture as source for drought-tolerant rootstocks, was used as source for the first cell line, and the second cell line was generated from the North American grape *V. riparia* that grows in alluvial forests and therefore is not adapted to drought. To test, whether the two lines differ in adaptation to salinity, we monitored the relative growth rate (using PCV as readout) under continuous challenge with three concentrations of NaCl (50, 85 and 155 mM) as shown in Fig. 1a, b. The cell lines differed clearly in their growth behaviour and in their response to salinity. Under control conditions, *V. rupestris* (Fig. 1a) steadily accelerated growth with a peak of 50 % daily volume increase at day 4, slowing down during the subsequent days. Already the lowest concentration of salt (50 mM) made the cells shrink initially and reduced growth rate during the first days. However, for 50 mM of salt, growth rate recovered subsequently and even strongly exceeded that of the control at day 6 (160 % daily volume increase). Even for 85 mM NaCl, growth rate recovered peaking at day 7 with a value of 40 % daily volume increase. This recovery contrasted with the situation observed in *V. riparia* (Fig. 1b). Here, under control conditions, growth rate increased to a peak of 40 % daily volume increase at day 2, slowly decreasing during the subsequent days. For treatment with 50 mM, the initial shrinkage could be compensated by a recovery of growth rate peaking at day 5 with 45 % daily volume increase. For 85 mM NaCl, no such recovery was observed. To test, whether the reduced salt adaptation of *V. riparia* correlated with a higher mortality (in percent), we scored at day 8 cells stained by the non-permeable dye Evans Blue (Gaff and Okong'O-Ogola, 1971). As shown in Fig. 1c, mortality at 50 and 85 mM NaCl was significantly increased in *V. riparia* over that found in *V. rupestris*, indicating a higher level of salinity-induced damage. However, these differences could not account for the reduced (50 mM NaCl) or lacking (85 mM NaCl) adaptation of growth rate in *V. riparia*. For the highest concentration used (155 mM NaCl), the majority of cells (~80 %) was dead in both cell lines, which explains the failure to recover growth rate. Thus, for 50 and 85 mM NaCl, *V. rupestris* displays a clear adaptation of growth after a lag of a few days, whereas this adaptive response is weaker (50 mM NaCl) or even absent (85 mM) in *V. riparia*.

The kinetics of Na⁺ uptake consist of three phases

To test the uptake of Na⁺ over time and to address the point, whether the different adaptation correlates with differences in uptake, the two cell lines were treated with 155 mM NaCl or with H₂O as a control and sampled at 2, 5, 10, 15, 30 min and 1, 2, 3 and 6 h to quantify Na⁺ ions. Figure 2a shows the time course of Na⁺ uptake and reveals that Na⁺ concentration does not increase at a constant rate. An initial phase I of rapid uptake is followed by a halting phase II (delineated by the

arrows in Fig. 2a) and a further phase III of rapid uptake. The early uptake (phase I) has been completed already at the first sampling point (2 min) and could not be resolved further due to the limitations in handling the samples. Interestingly, phase I results in a twofold higher Na⁺ content in *V. rupestris* (~6 mg/g) as compared to *V. riparia* (~3 mg/g). The two lines mainly differ in phase II: For *V. rupestris*, the concentration of salt oscillates around a steady-state level of ~7 mg/g and, from 10 min, even drops to 5 mg/g indicating that more Na⁺ is extruded from the cell than penetrates from outside (phase II). This process is subsequently fading and a new wave of salt increase initiates, such that Na⁺ concentration increases again to 8 mg/ml (phase III). In *V. riparia*, the halting phase II is barely manifest as a slower increase leading to a shoulder in the curve between 2 and 15 min. In contrast to *V. rupestris*, Na⁺ content is not dropping in phase II, but just growing slower. Finally, also for *V. riparia*, the cells “give in”, such that Na⁺ steadily increases arriving at the same final level as in *V. rupestris*.

Thus, the two lines differ in the timing of Na⁺ influx—whereas in the first 15 min Na⁺ levels are higher in *V. rupestris* than in *V. riparia*, this is reverted by active export of Na⁺ against a considerable concentration gradient. This export is so efficient in *V. rupestris* that, between 15 and 360 min, the salt concentration can be kept lower than in *V. riparia*.

Ca²⁺ influx alters Na⁺ uptake kinetics

Activation of Ca²⁺ influx channels located in the plasma membrane has been proposed as primary signal for salinity signalling (Knight et al. 1997). In addition, Ca²⁺ can block the NSCCs discussed as primary gate of Na⁺ influx (Demidchik and Tester 2002). We therefore tested the impact of external Ca²⁺ on Na⁺ uptake. Both cell lines were pretreated with 1 mM CaCl₂ directly before adding 155 mM NaCl (Fig. 2b, c). The effect of Ca²⁺ was qualitatively different depending on the respective phase of Na⁺ uptake: The increase of Na⁺ during the early phase I (<2 min) as well as during the intermediate phase II (2–15 min) was inhibited in both lines (more pronounced in *V. rupestris* than in *V. riparia*). In contrast, the uptake during phase III (>15 min) was promoted (more pronounced in *V. riparia* than in *V. rupestris*). To test which part of the Ca²⁺ effect is based on influx through the plasma membrane, GdCl₃ was used as bona fide inhibitor of both Ca²⁺ influx (Knight et al. 1997) and NSCCs (Demidchik et al. 2002) in a concentration that had been defined to be saturating for the inhibition of defence-related signalling in the same cell system (Qiao et al. 2010). Similar to treatment with exogenous Ca²⁺, the effect of GdCl₃ was dependent on the respective phase of salt uptake (Fig. 2d, e). During phase I, GdCl₃ reduced salt uptake slightly (similar to Ca²⁺). During phase II, the slope of uptake was higher than that observed for Ca²⁺. For phase III, GdCl₃ was

almost ineffective in *V. rupestris* (Fig. 2d), but clearly inhibitory in *V. riparia* (i.e. antagonistic to Ca^{2+} ; Fig. 2e).

Thus, the uptake of Na^+ can be dissected into at least two mechanisms that differ with respect to their dependency on external Ca^{2+} : The uptake before 15 min (phases I and II) is inhibited by Ca^{2+} (but also by GdCl_3 , indicating that Ca^{2+} influx is not the decisive factor here). In contrast, the uptake after 15 min (phase III) is promoted by Ca^{2+} (antagonized by GdCl_3 , indicating a role for Ca^{2+} influx channels).

Sign reversal in salt-induced changes of Ca^{2+} content

To interpret the Ca^{2+} effect on Na^+ uptake (Fig. 2b, c), we followed the time course of Ca^{2+} content during incubation with 155 mM NaCl. The time courses are shown in Fig. 3 and differ qualitatively between the two grapevine cell lines. In *V. rupestris* (Fig. 3a), Ca^{2+} content basically follows the temporal pattern of Na^+ uptake (Fig. 2a) with a rapid increase during phase I of Na^+ uptake, a plateau and a decrease during phase II and a second wave of increase in phase III of uptake. Since here only the Ca^{2+} in the MS medium (0.32 g/l CaCl_2) was available, potential release of cell-wall-bound Ca^{2+} should be equilibrated, such that these increases probably reflect the activity of Ca^{2+} influx channels. The pattern for *V. riparia* was basically a mirror image (Fig. 3a) with a sharp drop of Ca^{2+} during phase I of Na^+ uptake, a low plateau during phase II and a partial recovery during phase III. This means that, in *V. rupestris*, the pattern of Ca^{2+} content parallels that for Na^+ content, whereas in *V. riparia* the two ions show an inverted behaviour. This difference between the two cell lines represents a clear sign reversal.

Calcium content might change either by the activity of ion channels or by binding of Ca^{2+} ions to the pectic components of the cell wall. To discriminate between these two components, we repeated the time courses in the presence of GdCl_3 . For *V. rupestris*, the temporal pattern of Ca^{2+} content was not significantly altered by GdCl_3 (Fig. 3b), whereas for *V. riparia*, the Ca^{2+} content was strongly reduced (Fig. 3c). To probe for the contribution of Ca^{2+} binding to unsaturated pectic binding sites in the cell wall, in a third set of experiments, Ca^{2+} content was followed in the presence of either 1 mM CaCl_2 (to saturate binding sites in the cell wall), or of a combination of 1 mM CaCl_2 with 155 mM NaCl. In *V. rupestris*, incubation with 1 mM CaCl_2 established a high plateau of Ca^{2+} content within 2 min (about twofold as compared to 155 mM NaCl); this increase could be almost eliminated, when 155 mM NaCl was administered together with this Ca^{2+} treatment (Fig. 3d). In *V. riparia*, there was a distinct biphasic increase of Ca^{2+} content under these conditions. Prior to 15 min, 1 mM CaCl_2 alone caused a first wave of increase, which was followed from 15 min by a second rise leading to roughly the same Ca^{2+} levels as found in *V. rupestris* (Fig. 3e). When 155 mM NaCl was administered together with this high

Ca^{2+} content, there was virtually no difference to the situation observed for 155 mM NaCl alone. However, from 15 min, the Ca^{2+} levels increased parallel to the situation without NaCl, but to lower amplitudes. In summary, the two cell lines not only show a sign reversal with respect to Ca^{2+} levels in response to salinity but they also differ with respect to a late Ca^{2+} influx (>15 min) present in *V. riparia*, but not in *V. rupestris*, and probably with respect to the presence of free binding sites for Ca^{2+} in the cell wall.

NaCl-induced extracellular pH differs in both cell lines

Extracellular alkalinisation is considered to be one of the earliest defence-related responses as the apoplast is seen as the first plant compartment challenged by environmental signals (Felix et al. 1993; Hoson 1998). However, it is also an early signal in the response to salinity stress (Geilfuss and Mühling 2013). This response covers two underlying mechanisms—a rapid influx of Ca^{2+} and protons (Jabs et al. 1997), followed by an efflux of anion exporters that are activated by Ca^{2+} signalling (Felle et al. 1998). We therefore followed the response of extracellular pH [pH_{ext}] to salinity in the two cell lines as shown in Fig. 4. Both cultivars first showed a transient reduction of pH_{ext} recovering the initial level and then, from around 3 min after addition of salt, produced a strong alkalinisation that was maximal about 10 min later and then very slowly declining. The lag time for the initiation of proton transport was shorter in *V. rupestris* (15 s) as compared to *V. riparia* (36 s). *V. rupestris* cells also showed a more pronounced alkalinisation ($\Delta\text{pH}_{\text{ext}} \sim 0.4$) (Fig. 4a) as compared to *V. riparia* ($\Delta\text{pH}_{\text{ext}} \sim 0.25$) (Fig. 4b). To test the role of NSCCs on inducing pH_{ext} , GdCl_3 , as inhibitor of mechanosensitive Ca^{2+} influx channels, but also of NSCCs, was applied for 2 min before adding NaCl (Fig. 4a, b). GdCl_3 sharply reduced pH_{ext} of cells. This was followed by a slow, but steady increase of pH in *V. rupestris* restoring the initial level, whereas no such recovery was observed in *V. riparia*. Even when the concentration of GdCl_3 was increased to 0.75 mM in *V. rupestris*, pH_{ext} could recover partially. When GdCl_3 was administered in the absence of salinity, no recovery of pH was observed even in *V. rupestris*, indicating that this recovery resulted from the salt-induced alkalinisation on the background of a more acidic pH.

The comparison of Figs. 2 and 3 reveals that apoplastic pH decreases during the early phase I of rapid Na^+ uptake but increases preceding phase II of Na^+ uptake. This increase is more pronounced in *V. rupestris* (where during phase II even more Na^+ is extruded than enters the cells) as compared to *V. riparia* (where Na^+ uptake during phase II is just slowed down slightly). GdCl_3 delayed/ reduced salt-triggered alkalinisation in *V. rupestris* (Fig. 4a) and impaired the efficiency by which the uptake of Na^+ could be halted during phase II (Fig. 2d). In *V. riparia*, where GdCl_3 had almost no

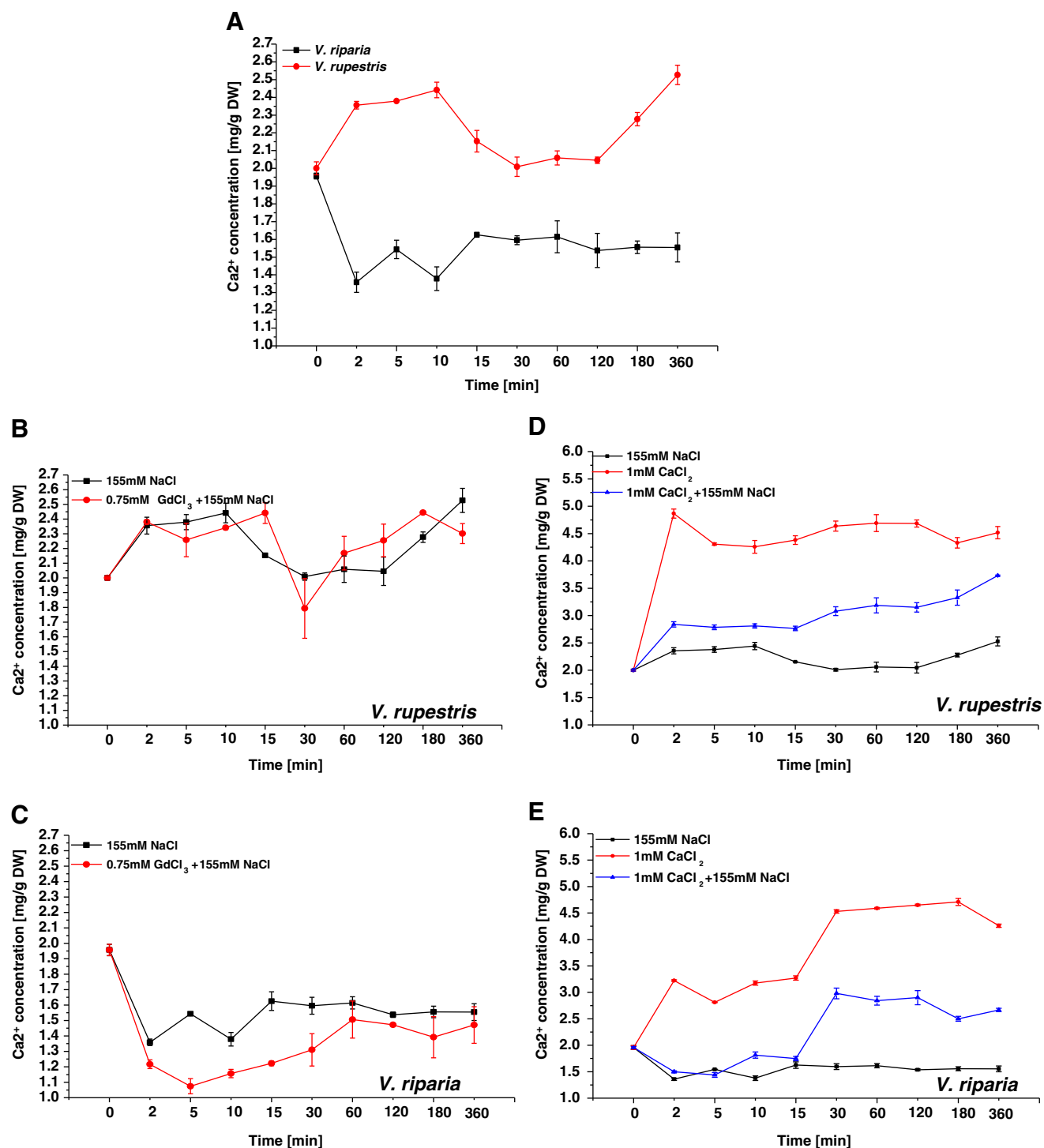


Fig. 3 Time course of Ca²⁺ uptake upon continuous challenge with 155 mM NaCl in control cells (**a**) of *V. rupestris* (red) versus *V. riparia* (black) and after pretreatment with 750 μ M GdCl₃ (**b, c**) or 1 mM CaCl₂ (**d, e**) for *V. rupestris* (**b, d**) and *V. riparia* (**c, e**). Data represent mean

values and standard errors from three independent experimental series. As negative control in **d** and **e**, Ca²⁺ content after Ca²⁺ application was followed (red lines). To resolve the early time point, the time axis is plotted in a non-linear scale

effect on Na⁺ uptake (Fig. 2e), salt-triggered alkalinisation was completely suppressed (Fig. 4b). Thus, there is a correlation between phase II of Na⁺ uptake and the amplitude/robustness of extracellular alkalinisation.

Phytohormones accumulate differently during salinity stress

To clarify the role of the JA pathway in comparison to the adaptive role of ABA, endogenous levels of JA, JA-II and

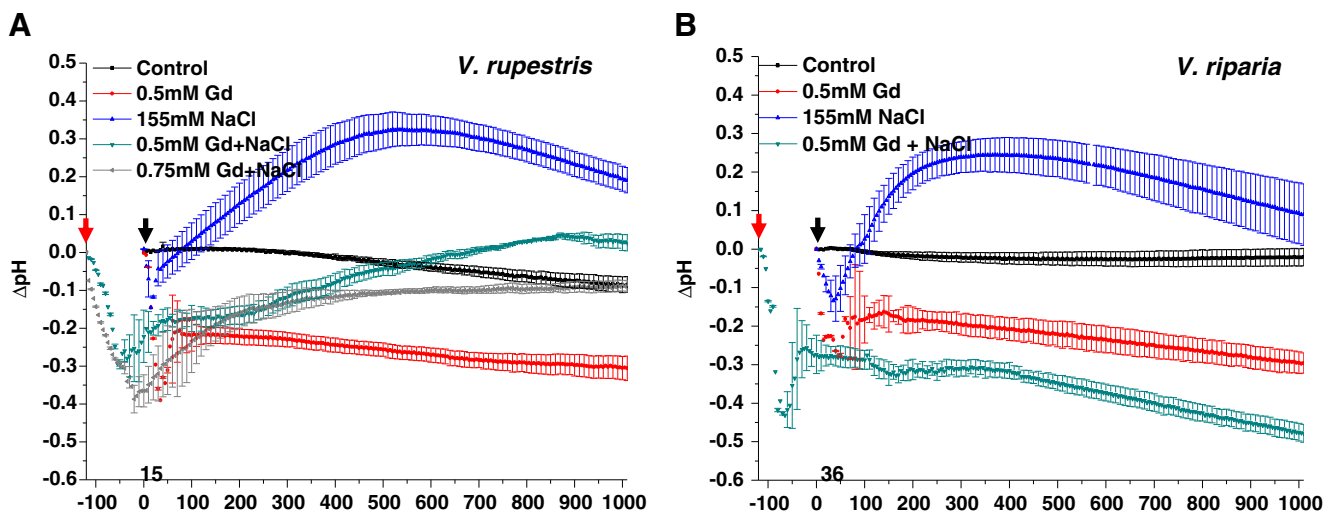


Fig. 4 Representative time course of the response of apoplastic pH to 155 mM NaCl alone or after adding 0.5 and 0.75 mM of GdCl₃ (an inhibitor of NSCCs) for 2 min for *V. rupestris* (a) or *V. riparia* (b). Red-

coloured arrow for adding GdCl₃ before NaCl was applied after 2 min (black-coloured arrow). Values are means \pm SE (n =at least 3)

ABA were followed in response to 155 mM NaCl in cells at day 5 after subcultivation as shown in Fig. 5. For JA, the ground level in *V. riparia* was more than twice of that found in

V. rupestris and increased further by about 25 % from 3 h after the onset of salt treatment (Fig. 5a). In contrast, *V. rupestris* maintained a very low level of JA, even after prolonged

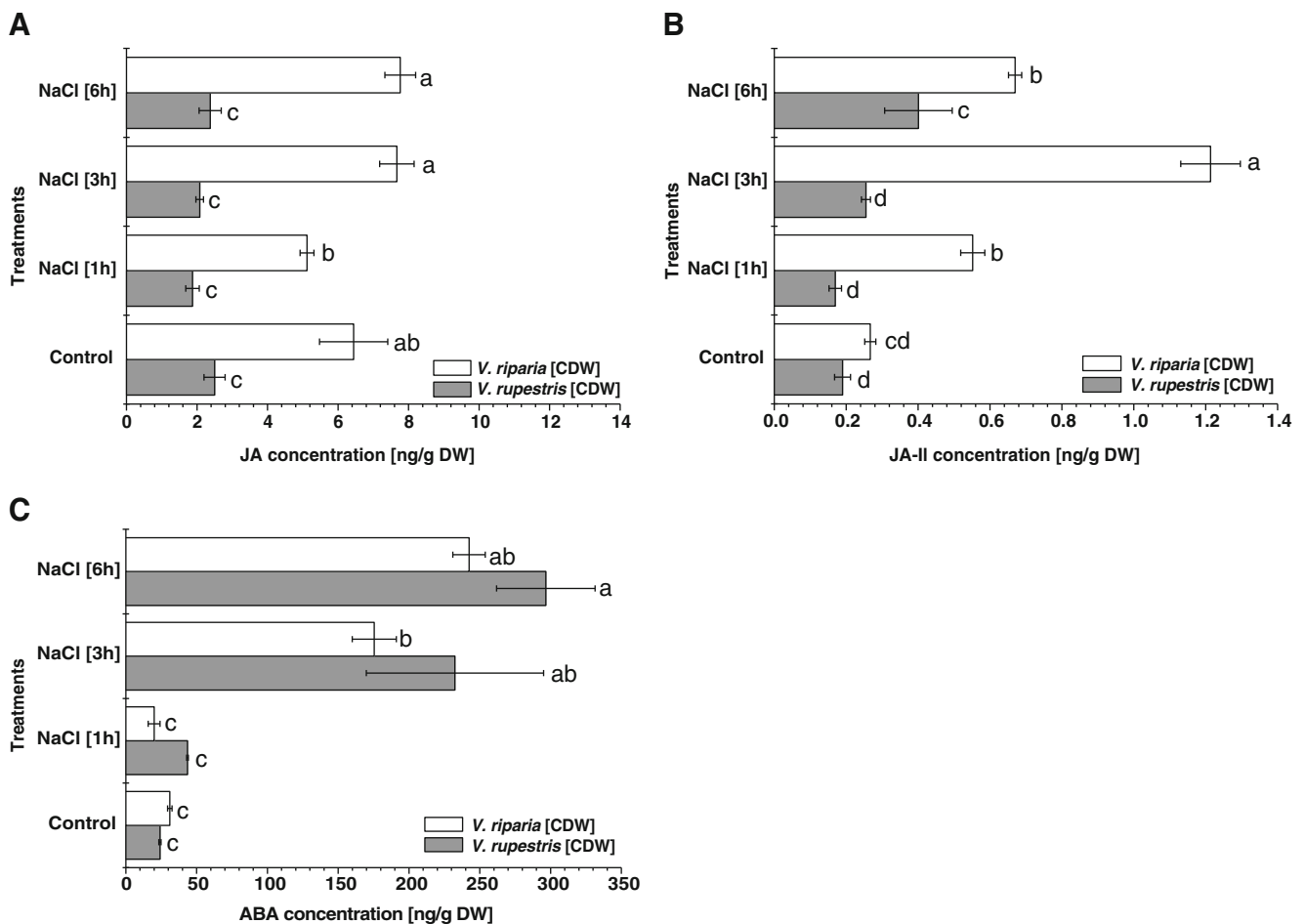


Fig. 5 Representative time course of endogenous JA (a), JA-II (b) and ABA (c) under 155 mM NaCl at 1, 3 and 6 h in both cell lines. Control samples were treated by H₂O for 1 h. Error bars represent SE, and different letters indicate significant differences among treatments (LSD (P <0.05))

salinity. The difference was even more pronounced, when the highly bioactive JA-II was measured (Fig. 5b). Here, salt induced a fourfold increase for *V. riparia*, whereas *V. rupestris*, after 6 h of salt stress, had just reached the level of JA-II found in unchallenged control cells of *V. riparia*. For ABA (Fig. 5c), the situation was reversed—here, in *V. rupestris*, the induction was more pronounced as compared to *V. riparia*, although both lines accumulated comparable levels of ABA from 3 h after the onset of treatment. Thus, the improved salinity adaptation in *V. rupestris* correlated with a clear reduction in salt-induced formation of JA and most pronounced JA-II. In contrast to JA, IAA and SA were much higher in unchallenged *V. rupestris* as compared to *V. riparia* (supplemental Fig. 3A, B). Salinity made both hormones decline in *V. rupestris*, whereas in *V. riparia* there was no significant change.

Sign reversal in calcium effect on salt-induced hormone levels

Since the two cell lines showed qualitative differences in Ca^{2+} accumulation (Fig. 3), we investigated the effect of either GdCl_3 or CaCl_2 on salt-induced accumulation of phytohormones as shown in Fig. 6. In *V. riparia*, 0.75 mM of GdCl_3 triggered a strong accumulation of JA and JA-II within 1 h (Fig. 6a, b). When salt was combined with the GdCl_3 treatment, this progressively quelled the GdCl_3 triggered increase such that the JA and JA-II levels from 3 to 6 h after induction had returned to the ground levels (Fig. 6a, b), whereas they remained elevated when the salt treatment was administered in the absence of GdCl_3 (Fig. 5a, b). Similar to GdCl_3 , 1 mM CaCl_2 increased the ground levels of JA and JA-II. For ABA, neither GdCl_3 nor CaCl_2 caused any significant accumulation (Fig. 6c). Moreover, the salt-induced accumulation of ABA (Fig. 5c) was suppressed by GdCl_3 . In *V. rupestris*, where JA did not accumulate in response to salt (Fig. 5a), GdCl_3 and CaCl_2 reduced the level of JA (Fig. 6a) and JA-II (Fig. 6b) even further; however, GdCl_3 significantly increase the accumulation of JA-II after 3 h in response to salt. In the same line, the level of ABA was not elevated in *V. rupestris* by GdCl_3 as well as by CaCl_2 , but the strong accumulation of ABA in response to salt in this cell line (Fig. 5c) was even further promoted by GdCl_3 (Fig. 6c). In summary, the response of salinity-triggered accumulation of JA/JA-II shows differential sensitivity to GdCl_3 between the two cell lines, and for salinity-triggered accumulation of ABA, there is even a sign-reversal.

A pretreatment with GdCl_3 cancelled the salt-induced decrease of IAA and SA in *V. rupestris* (compare supplemental Fig. 3A, B with supplemental Fig. 4A, B). However, IAA was significantly induced when GdCl_3 was applied alone or with NaCl for 1 h. In contrast, *V. riparia* displayed no changes in both hormones comparing to NaCl alone. CaCl_2 , on the other hand, resulted in IAA reduction only after 3 h of application *V. rupestris* (supplemental Fig. 4A, B).

Stilbene accumulation in response to salt

In grapevine, the accumulation of stilbenes represents an important event in defence. For the grapevine cell system used in the current study, especially the accumulation of the highly cytotoxic δ -viniferin has been shown to herald defence-related cell death (Chang et al. 2011). Since defence-related signalling and salinity-induced signalling share several events (Ismail et al. 2012), we used salinity triggered accumulation of stilbenes as indicator for damage-related signalling. Figure 7 shows the accumulation of the stilbene-glycoside α -piceid (Fig. 7a), the aglycone *trans*-resveratrol (Fig. 7c) and the highly toxic oxidative dimer δ -viniferin (Fig. 7b) in response to salinity. Salt-stressed *V. riparia* cells accumulated piceid in levels comparable to the piceid triggered preceding defence-related PCD (Chang and Nick 2012). In contrast, *V. rupestris* did not accumulate α -piceid (Fig. 7a). *V. riparia* cells also accumulated δ -viniferin (the toxic oxidative dimer of resveratrol) whereas *V. rupestris* cells did not (Fig. 7b). Compared to the situation in defence-related cell death (Chang and Nick 2012), the levels of salt-induced δ -viniferin were lower, however (around 15 %). For *trans*-resveratrol, only very low levels (around 0.020–0.030 $\mu\text{g/g}$) were measured with higher accumulation in *V. riparia* (Fig. 7c), which is about two orders of magnitude lower than the values obtained for defence-related cell death (Chang and Nick 2012). These results show that *trans*-resveratrol is almost absent under salinity stress. Furthermore, the stilbene pattern for salinity (α -piceid, δ -viniferin) differs from that for defence-related cell death (*trans*-resveratrol, δ -viniferin). Finally, stilbene output (a response to oxidative stress, see Chang and Nick 2012) is quelled in *V. rupestris*, but not in *V. riparia*.

Discussion

To disentangle plant stress signalling represents a scientific challenge: Numerous events overlap between *stress adaptation* and *stress damage*, on one hand, and the large number of only partially identified players make it difficult to delineate a clear-cut line between both events, on the other hand. In the present work, we investigated, in parallel, two grapevine cell lines differing in their performance under salinity. Our basic approach was to correlate differences of early salinity-induced responses with the differential adaptation of the two cell lines. This should allow to assign these events to either *stress adaptation* or *stress damage*.

The faster the early response, the better the adaptation

We observed that the fluxes of Na^+ (resulting in stress damage) and Ca^{2+} and H^+ (acting as stress signals) proceeded in both lines, however, with different spatiotemporal pattern

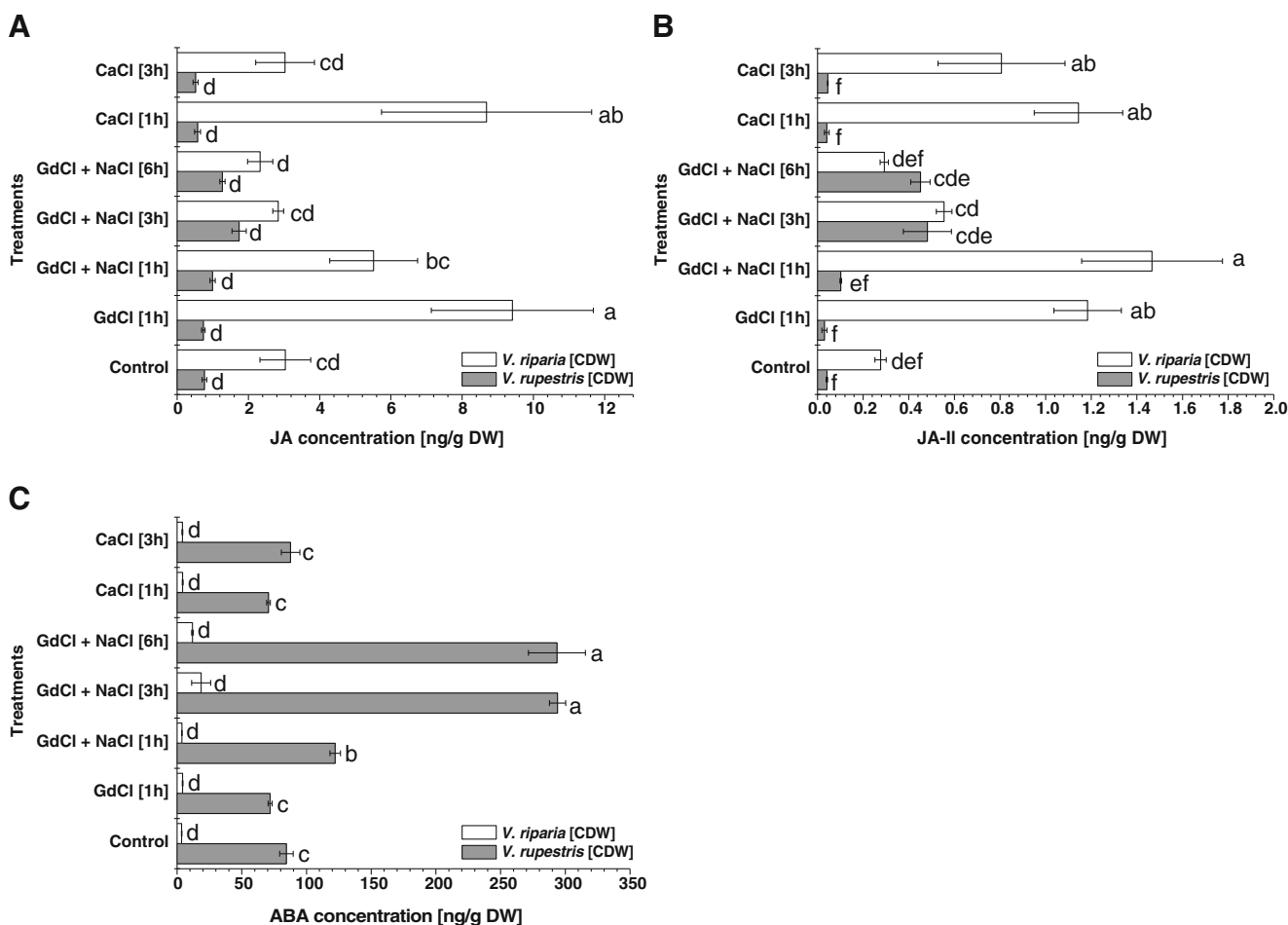


Fig. 6 Endogenous JA (a), JA-II (b) and ABA (c) under different treatments at different time points in *Vitis* cells elicited by 155 mM NaCl after 0.75 mM of GdCl₃ pretreatment for 2 min or by 1 mM CaCl₂ alone

for 1 and 3 h. Control samples were treated by H₂O or 0.75 mM of GdCl₃ for 1 h. Error bars represent SE, and different letters indicate significant differences among treatments (LSD ($P < 0.05$))

(signatures). When Na⁺ ions are administered to a plant, they enter by passive transport through the plasma membrane NSCCs (mainly DA-NSCCs and VI-NSCCs) within seconds (Tester and Davenport 2003). The two studied cell lines showed different Na⁺ flux pattern (Fig. 2a). Since the elevated intra- and extracellular Na⁺ partially inhibits the K⁺ outward rectifiers, the higher initial uptake of Na⁺ during phase I in *V. rupestris* might prevent the loss of cellular K⁺, maintaining cellular K⁺/Na⁺ homeostasis under stress (Shabala et al. 2006). The rapid uptake of Na⁺ in *V. rupestris* during phase I would also contribute to overcome osmotic loss of water (Munns and Tester 2008) and might contribute to the pronounced drought tolerance of this species.

The earliest cellular response to salinity seems to be a rapid increase of free cytosolic Ca²⁺ within 1 to 5 s either through influx channels situated in the plasma membrane or through release from internal stores, especially the vacuole (Donaldson et al. 2004; Knight et al. 1997). Interestingly, *V. riparia* exhibited a sharp drop of cellular Ca²⁺ content concomitantly with phase I of Na⁺ uptake (Fig. 3a) consistent with a release of Ca²⁺ from the apoplast. A similar decrease of

cellular Ca²⁺ content had been described for mesophyll tissue of *Vicia faba* L. leaves and for barley roots, but was absent in protoplasts derived from these cells, a phenomenon which was attributed to Na⁺/Ca²⁺ and H⁺/Ca²⁺ ion exchange in the cell wall (Cuin and Shabala 2005; Shabala and Newman 2000). A pretreatment with GdCl₃ even amplified this salt-induced Ca²⁺ drop as compared to NaCl alone (Fig. 3c). This inhibitor experiment suggests that a certain salinity-induced Ca²⁺ influx does exist. However, it seems to proceed with low efficiency and is overrun by the Ca²⁺ loss from the cell wall. In fact, when excess Ca²⁺ was applied alone or in combination with NaCl to saturate binding sites in the cell wall, Ca²⁺ influx became visible in *V. riparia* but its activity was low (Fig. 3e) correlated with a low rate of Na⁺ and H⁺ influx under salt stress (Figs. 2a and 4b).

In contrast, the pattern of Ca²⁺ influx in NaCl-treated *V. rupestris* showed a mirror image: Here Ca²⁺ content changed in a manner similar to Na⁺ uptake, with a clear induction in the first 10 min. This correlates with the kinetic efficacy of NSCCs and their fast uptake of both Na⁺ (Fig. 2a) and H⁺ (Fig. 4a), which might sequester them from occupying

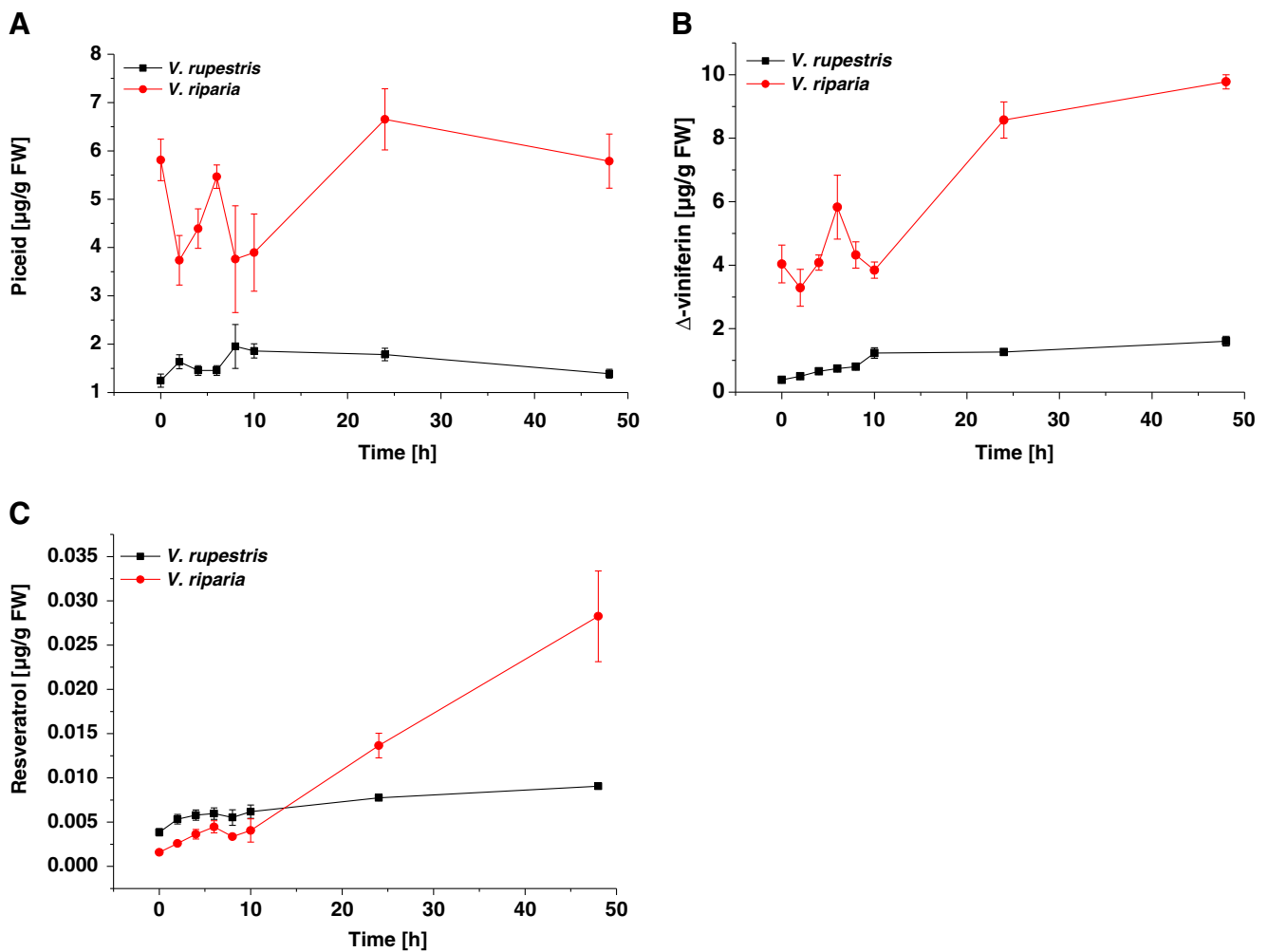


Fig. 7 Grapevine stilbenes under salinity. The induction of piceid (a), δ -viniferin (b) and resveratrol (c) (in micrograms per gram) in response to 155 mM NaCl in both cell lines at different time points. Values are means \pm SE ($n=3$)

potential Ca^{2+} -binding sites in cell wall. This effect would be complemented by a more efficient influx of apoplastic Ca^{2+} into the cytoplasm (Fig. 3a, b, d). Similar to the elevated Na^+ uptake during phase I, this fast Ca^{2+} uptake might be linked to the pronounced drought tolerance of *V. rupestris* and thus be correlated more with osmotic rather than ionic stress (Knight et al. 1997).

Salinity-induced cytosolic Ca^{2+} , in turn, activates the plasma membrane ATPases mediated by Ca^{2+} -CaM-dependent protein kinases, restoring membrane voltage after Na^+ -induced depolarization and maintaining membrane integrity and ionic homeostasis (Klobus and Janicka-Russak 2004; Shabala et al. 2006). Additionally, the elevated cytosolic Ca^{2+} promotes H^+ influx and inhibits AHA1 (a P-type proton ATPase catalyzing H^+ efflux) resulting in apoplastic alkalisation (Wolf et al. 2012). Kinetic differences in cytosolic Ca^{2+} spiking should therefore become manifest as kinetic differences of apoplastic pH. In fact, salt stress induces a rapid apoplastic alkalisation that differs between the two cell lines with respect to kinetics and dose dependency (Ismail

et al. 2012). Consistent with the more active early Ca^{2+} influx in response to NaCl (155 mM), the lag time for apoplastic alkalisation was only 15 s in *V. rupestris*, whereas the sluggish Ca^{2+} influx in *V. riparia* was correlated with a longer lag of alkalisation of 36 s (Fig. 4). As to be expected, salinity-induced Ca^{2+} fluxes act upstream of proton fluxes. The lanthanoid GdCl_3 completely blocked (*V. riparia*) or at least impaired (*V. rupestris*) apoplastic alkalisation. Cytoskeleton-tethered mechanosensors participate in the perception of osmotic stress signals (Türkan and Demiral 2009) and trigger a rapid increase of cytosolic Ca^{2+} within 1 s, followed by apoplastic alkalisation within 12 s. Both ion fluxes are blocked by a pretreatment with the lanthanoid La^{3+} (Monshausen et al. 2009). Thus, the earliest events of the cellular salinity response are shared with those triggered by mechanic challenge. Additionally, the Ca^{2+} -induced H^+ influx might feedback on Ca^{2+} signalling by affecting Ca^{2+} affinity for CaM (Busa and Nuccitelli 1984). Apoplastic alkalisation might promote adaptive events including activation of wall-consolidating enzymes such as pectin methylesterase or, on

the other hand, inhibition of expansins involved in cell-wall expansion (Wolf et al. 2012). In *V. rupestris*, alkalinisation was much more pronounced ($\Delta\text{pH}_{\text{ext}} \sim 0.4$) (Fig. 4a) compared to *V. riparia* ($\Delta\text{pH}_{\text{ext}} \sim 0.25$) (Fig. 4b) suggesting that adaptive arrest of cell expansion may underlie the initial decrease of growth rates in NaCl-stressed *V. rupestris* in contrast to *V. riparia* (Fig. 1a, b).

As additional adaptive event, the salt-induced free cytosolic Ca^{2+} promotes the SOS3/SOS2 which phosphorylates the membrane-bound Na^+/H^+ antiporter, SOS1 causing Na^+ efflux (Qiu et al. 2002). The more efficient Ca^{2+} uptake in *V. rupestris* should therefore cause a subsequent decline in cellular Na^+ content, which would be a mechanistic explanation for the drop in Na^+ content during phase II (Fig. 2a). Since SOS2 also regulates the vacuolar Na^+ transporter NHX1, in concert with other members of this family of transporters maintaining Na^+ and K^+ homeostasis even under drought and salt stress (Apse et al. 1999; Gaxiola et al. 1999; Qiu et al. 2004), the more active Ca^{2+} influx in *V. rupestris* should be followed by induction of NHX1 transcripts. In fact, in our previous work, we found strong induction of NHX1 transcripts after 3 h of salinity stress in *V. rupestris*, but not in *V. riparia* (Ismail et al. 2012). The induction of the vacuolar NHX1 transporter in conjunction with the sensitivity of Na^+/H^+ antiporters to cytosolic pH (Padan et al. 2001) indicates that, in *V. rupestris*, the Na^+ entering the cell during phase III of uptake is efficiently compartmentalized into the vacuole, whereas in *V. riparia*, more Na^+ would remain trapped in the cytoplasm.

On the other side, elevated levels of apoplasmic Ca^{2+} strongly and partially block the main gates of Na^+ entry, VI-NSCCs and DA-NSCCs, respectively (Demidchik and Maathuis 2007). When external Ca^{2+} was added to the *Vitis* cells, it significantly reduced Na^+ influx in both cell lines, with higher efficacy in *V. rupestris* (Fig. 2b, c). However, this positive effect was reverted in phase III, where Ca^{2+} significantly increased Na^+ uptake in both cell lines, especially in *V. riparia*. Since the two lines showed different Ca^{2+} influx pattern under all treatments (Fig. 3), elevated levels of cytosolic Ca^{2+} at the beginning of phase III (from 15 min) in both cell lines might activate the HA-NSCCs that are weakly selective for monovalent cations with a late activation ~40–60 min (Davenport and Tester 2000; Demidchik et al. 2002). Again, when GdCl_3 was applied 2 min before salt treatment, Na^+ uptake was reduced during both phases I and II in both lines (being less effective than Ca^{2+}). However, unlike the Ca^{2+} signature, this inhibitory effect was pronounced during phase III only in *V. riparia*, but absent in *V. rupestris* (Fig. 2d, e). In *Arabidopsis* root epidermal protoplasts, already 100 μM GdCl_3 was sufficient to suppress 95 % of Ca^{2+} influx carried by HA-NSCCs (Demidchik et al. 2002) indicating that the HA-NSCCs may be the predominant type of channels on *V. riparia* plasma membranes. In contrast, the

two more effective NSCCs (DA-NSCCs and VI-NSCCs) might represent the major type of channels in *V. rupestris*. This work hypothesizes the apparent strong impact of plasma membrane NSCCs and their kinetic activities on the early stress responses of plants which have to be tested through electrophysiological approaches. Since these channels transport Ca^{2+} and H^+ and thus determine the signatures of these signals, NSCCs activity acts upstream of Ca^{2+} and H^+ flux and signalling activity and thus represent the earliest events of adaptive signalling.

The tighter the control of JA/JA-II accumulation, the better the adaptation

ABA and JAs play central roles in plant adaptation to stress, constraining root growth, cell cycle, photosynthesis and transpiration, and thus prioritizing defence metabolism over growth. Furthermore, they play essential and overlapping roles for the induction of stomatal closure (Suhita et al. 2004). Upon osmotic stress, ABA accumulates resulting in upregulation of osmotic stress-responsive genes such as the ABA-responsive element/complex (Ishitani et al. 1997). This ABA accumulation is clearly adaptive, since the ABA deficient *aba*-mutants of *Arabidopsis* perform poorly under drought or salt stress or even die (Zhu 2002). However, ABA seems to be not the only adaptive signal. ABA-deficient mutants of maize and tomato showed generally the same leaf growth rates as wild-type plants in drying or saline soils, and *Arabidopsis DREB1A* and its functional rice ortholog *OsDREB1A* promote tolerance to drought, high-salt and freezing stresses independently of ABA (Dubouzet et al. 2003). As candidate for this ABA-independent signal, gibberellins have been suggested (Munns and Tester 2008). However, recently, *OsDREB1A* was found to be upregulated downstream of *OsbHLH148* in a JA-dependent fashion, whereby *OsbHLH148* is suppressed by *OsJAZs* (especially *OsJAZ1* and 3). Under JA signalling, *OsbHLH148*, *OsJAZ* and *OsCOI1* assemble into a complex resulting in the degradation of *OsJAZ* proteins via the 26S proteasome and thus the release of *OsbHLH148* (Seo et al. 2011).

In the current study, the two cell lines accumulated comparable levels of ABA (Fig. 5c). However, in the salt-sensitive *V. riparia*, the accumulation of JA and JA-II was fourfold and sixfold, respectively, as compared to the more osmotic-tolerant *V. rupestris* (Fig. 5a, b). Moreover, in *V. riparia*, JA-II was induced earlier (after 1 h), while in *V. rupestris* 6 h was required until a first significant induction became visible and even then just reached the ground level of JA-II observed in *V. riparia*. Synthesis and accumulation of JA have been linked with PCD in infected tobacco leaves (Kenton et al. 1999) and *Arabidopsis* protoplasts (Zhang and Xing 2008) and both leaves and cell-suspension cultures of *Vitis vinifera* L. cv. Lemberger (Repka et al. 2004). Interestingly,

JA does not promote PCD only in plant cells but also in cancer cells and sharing several similar effects in both cells including ROS generation, MAPK induction, cell cycle arrest and PCD (Flescher 2007). In the *V. rupestris* cell line, the elicitation of cell death by the bacterial effector Harpin was preceded by accumulation of both resveratrol and its toxic oxidative dimer δ -viniferin (Chang and Nick 2012). However, the same line produced very little of these stilbenes in response to salinity stress (Fig. 7). In contrast, salt-stressed *V. riparia* cells accumulated high amounts of δ -viniferin following the accumulation of JA and JA-II (Fig. 7b). In our previous work, we could show that a pronounced oxidative burst is observed in *V.*

riparia peaking at 1 h, which is absent in *V. rupestris* (Ismail et al. 2012). The findings from the current and our previous (Ismail et al. 2012) study link salt tolerance in *V. rupestris* with suppression of oxidative burst, reduced accumulation of JA and JA-II, early induction of *JAZ1*, induction of *NHX1*, suppression of stilbene accumulation and reduced cell death. In contrast, the salt-sensitivity of *V. riparia* is linked with an early oxidative burst, massive accumulation of JA and JA-II, accumulation of stilbenes and cell death, whereas induction of *JAZ1* transcripts and *NHX1* is suppressed. Since MeJA (10 μ M) promotes the accumulation of *cis*- and *trans*-resveratrol and their glycosides, piceid, in *V.*

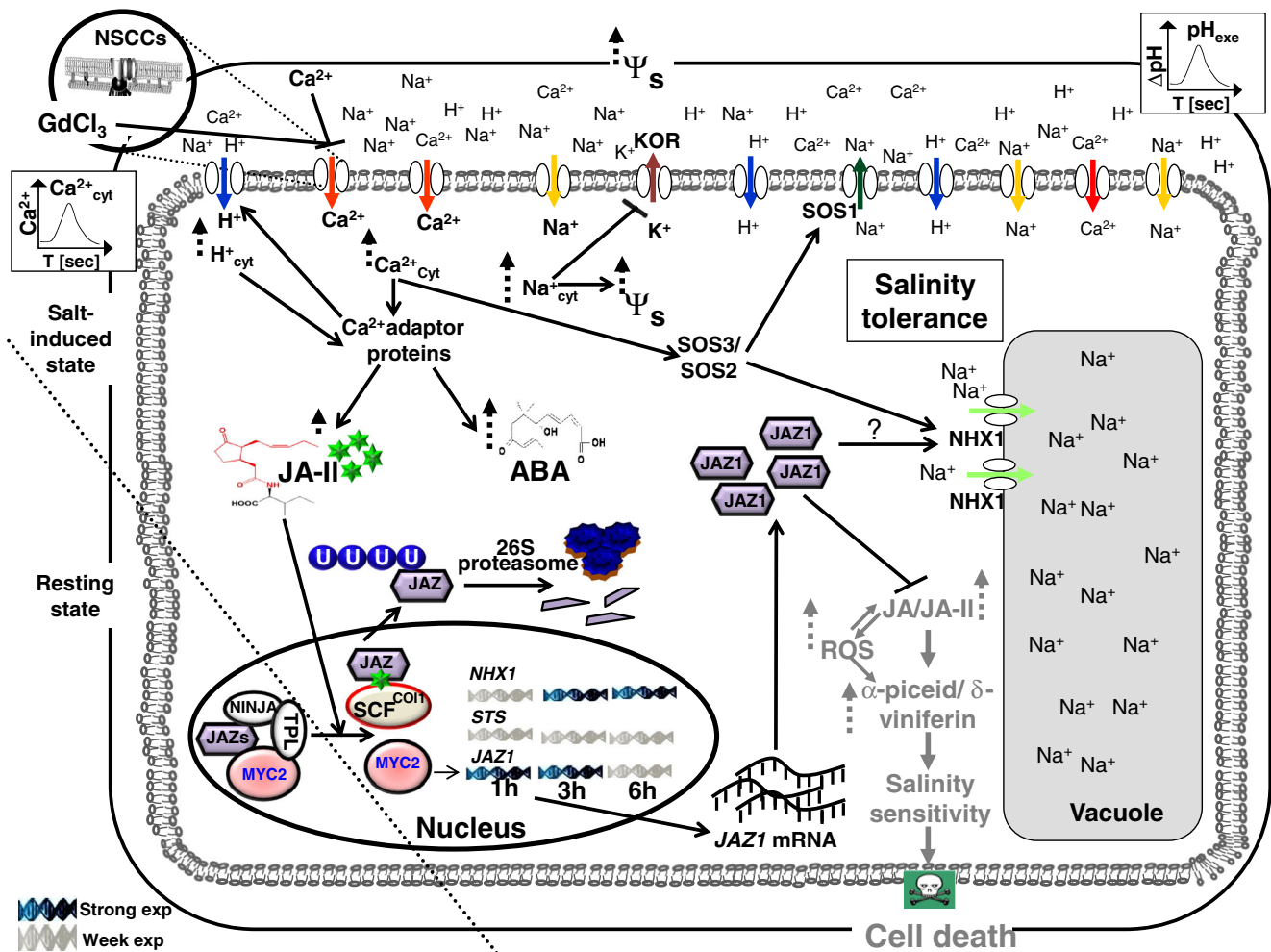


Fig. 8 Model for salinity tolerance or sensitivity: In the control situation, JA signalling is suppressed by a multimeric transcriptional corepression complex (JAZ/TIFY, TPL, TPRs and NINJA). However, upon salinity stress, fluxes of Na^+ , Ca^{2+} and H^+ occur with different spatiotemporal signatures channelling plant cells to either salinity adaptation or cell death. Details are given in the discussion. Coloured and black arrows indicate activation by salinity stress and internal triggers, respectively. On the plasma membrane, arrows with blue, red and orange represent H^+ , Ca^{2+} and Na^+ influx, while dark green and brown show Na^+ and K^+ efflux, respectively. Light green arrows represent Na^+ influx into vacuole. Dashed arrows (\blacktriangle , \blacktriangleright , \blacktriuparrow)

refer to non-significant (later significant after 6 h), significant and highly significant induction. Black arrows indicate activated signalling pathways while gray ones for inactivation. Black lines indicate repression action. ABA abscisic acid, JA jasmonic acid, JA-II jasmonoyl isoleucine, ROS reactive oxygen species, SA salicylic acid, STS stilbene synthase, Ψ_s osmotic potential, KOR K^+ outward rectifiers, NSCCs non-selective cation channels, SOS salt overly sensitive, *NHX1* vacuolar Na^+/H^+ exchanger 1, *JAZ1* jasmonate ZIM-domain protein 1, *TPL* the corepressor TOPLESS, *TPRs* TPL-related proteins, *NINJA* a novel interactor of JAZ (NINJA), *U* ubiquitination

vinifera cell suspension (Krisa et al. 1999; Tassoni et al. 2005). Resveratrol, in turn, can efficiently induce, in grapevine suspension cells, oxidative burst, actin bundling, accumulation of cell-death-related PR5 and cell death (Chang et al. 2011), suggesting that the JA pathway triggers PCD via stilbenes. It should be noted that the jasmonate responses discussed here occur early after challenge by salinity and clearly meet the criteria of *stress damage*. The role of jasmonate during later phases (*stress adaptation*) can be different and remains to be elucidated. This is indicated by our previous finding (Ismail et al. 2012) that exogenous jasmonate can promote the re-initiation of growth in *V. riparia* at day 4 after the onset of salinity stress by priming the JAZ transcription.

This leads to a model, where constrained JA accumulation and signalling are a precondition to escape salinity-induced cell death and to activate salinity adaptation. As expected from this model, the JAZ proteins as negative regulators of JA signalling are crucial for the tolerance salinity and drought: When GsJAZ2 from *Glycine soja* was over-expressed in *Arabidopsis*, the resultant mutant performed better than wild type under salinity with a significant accumulation of NHX1 after 6 h (Zhu et al. 2012). Furthermore, in a rice mutant over-expressing OsBHLH148, both OsDREB and OsJAZ genes were highly induced upon drought stress (Seo et al. 2011). Over-expression of OsJAZ9 significantly improved salt and drought tolerance of rice (Ye et al. 2009). Taken together, the accumulated data strongly pointed to the key roles of JAZ proteins in improving salinity stress tolerance by fine tuning JAs signalling and tightly control JAs levels. Of course, the crucial roles of JAs in improving salinity or drought stress, such as inducing stomatal closure, OsBHLH148 activity and even the induction of JAZ genes, cannot be ignored. However, the existence of efficient re-suppression machinery, like JAZ proteins, that tightly control JAs levels should be considered as stress determining factor. The accumulation of JA, JA-II and ABA depends on Ca^{2+} homeostasis, since in *V. riparia* both excessive Ca^{2+} as well as inhibition of Ca^{2+} influx by GdCl_3 can induce JA and JA-II in the salt-sensitive *V. riparia*, whereas in the salt-tolerant *V. rupestris* GdCl_3 induces ABA instead with some cross-talk on the accumulation of SA (supplemental Figs. 3 and 6). Calcium homeostasis might be the factor that links the early salinity-induced events (ion-fluxes, apoplastic alkalinisation) with later events of *stress damage* (JA, JA-II, stilbenes, dominating in *V. riparia*) versus *stress adaptation* (ABA, SA, NHX1, dominating in *V. rupestris*).

Towards a model for salinity tolerance or sensitivity

In the current study, we addressed the role of JA signalling in the context of salinity stress. As biological template to assign the investigated cellular events to either salt damage or salt adaptation, we compared two grapevine cell lines differing in

their ability for salt adaptation. The successful adaptation to salinity stress in *V. rupestris* is correlated with an efficient extrusion of Na^+ during phase II (between 2 and 15 min) accompanied by apoplastic alkalinisation. This is followed by accumulation of ABA, whereas the accumulation of JA and JA-II was quelled. As a consequence, stilbenes that accumulate in this system in the context of oxidative burst and PCD are suppressed. In contrast, the sensitive *V. riparia* is less efficient in the export of Na^+ during phase II correlated with a lower activity of apoplastic alkalinisation. Subsequently, JA and especially JA-II accumulate as well as the highly cytotoxic oxidative stilbene dimer δ -viniferin. Our data show clearly that JA and especially the biologically potent JA-II accumulate in the context of salt damage and are quelled in the context of salt adaptation. Figure 8 summarizes, on the phenomenological level, some of positive or negative events (Figs. 2, 3, 4, 5, 6 and 7 and supplemental Figs. 1, 2 and 3) that accompany salt adaptation in *V. rupestris* or salt sensitivity in *V. riparia*, respectively.

Since several players relevant for the uptake of sodium and the adaptation to Na^+ stress such as VI-NSCCs, DA-NSCCs, HA-NSCCs and SOS are regulated by Ca^{2+} , we probed the individual salinity-triggered events with respect to their modulation by exogenous Ca^{2+} or gadolinium ions as bona fide inhibitors of Ca^{2+} channels (Demidchik and Maathuis 2007; Knight et al. 1997). Moreover, we followed the changes of cellular calcium content in response to salinity. This “calcium/gadolinium signature” derived from these experiments can now be used as phenomenological framework to test molecular candidates and to assign their function to early and late events of *stress damage* versus *stress adaptation*.

Acknowledgments Authors gratefully acknowledge Dr. Yusuke Jikumaru for his support of hormone analysis. Gesine Preuss is acknowledged for Na^+ and Ca^{2+} measurements. Ahmed Ismail was supported by the German Egyptian Research Long term Scholarship “GERLS” programme.

References

- Apel K, Hirt H (2004) Reactive oxygen species: metabolism, oxidative stress, and signal transduction. *Annu Rev Plant Biol* 55:373–399
- Apse MP, Aharon GS, Snedden WA, Blumwald E (1999) Salt tolerance conferred by overexpression of a vacuolar Na^+/H^+ antiport in *Arabidopsis*. *Science* 285:1256–1258
- Babourina O, Leonova T, Shabala S, Newman I (2000) Effect of sudden salt stress on ion fluxes in intact wheat suspension cells. *Ann Bot* 85: 759–767
- Browse J (2009) Jasmonate passes muster: a receptor and targets for defense hormone. *Annu Rev Plant Biol* 60:183–205
- Busa WB, Nuccitelli R (1984) Metabolic regulation via intracellular pH. *Am J Physiol* 246:R409–R438
- Chang X, Heene E, Qiao F, Nick P (2011) The phytoalexin resveratrol regulates the initiation of hypersensitive cell death in *Vitis* cell. *PLoS ONE* 6(10):e26405. doi:10.1371/journal.pone.0026405

- Chang X, Nick P (2012) Defence signalling triggered by Flg22 and Harpin is integrated into a different stilbene output in *Vitis* cells. PLoS ONE 7:e40446. doi:10.1371/journal.pone.0040446
- Chini A, Fonseca S, Fernández G, Adie B, Chico JM, Lorenzo O, García-Casado G, López-Vidriero I, Lozano FM, Ponce MR, Micol JL, Solano R (2007) The JAZ family of repressors is the missing link in jasmonate signalling. Nature 448:666–671
- Creelman RA, Mullet JE (1995) Jasmonic acid distribution and action in plants: regulation during development and response to biotic and abiotic stress. Proc Natl Acad Sci U S A 92:4114–4119
- Cuin TA, Shabala S (2005) Exogenously supplied compatible solutes rapidly ameliorate NaCl-induced potassium efflux from barley roots. Plant Cell Physiol 46:1924–1933
- Davenport RJ, Tester M (2000) A weakly voltage-dependent, nonselective cation channel mediates toxic sodium influx in wheat. Plant Physiol 122:823–834
- Demidchik M, Tester M (2002) Sodium fluxes through nonselective cation channels in the plasma membrane of protoplasts from *Arabidopsis* roots. Plant Physiol 128:379–387
- Demidchik V, Bowen HC, Maathuis FJM, Shabala SN, Tester MA, White PJ, Davies JM (2002) *Arabidopsis thaliana* root non-selective cation channels mediate calcium uptake and are involved in growth. Plant J 32:799–808
- Demidchik V, Maathuis FJM (2007) Physiological roles of nonselective cation channels in plants: from salt stress to signalling and development. New Phytol 175:387–404
- Derckel JP, Baillieul F, Manteau S, Audran JC, Haye B, Lambert B, Legendre L (1999) Differential induction of grapevine defences by two strains of *Botrytis cinerea*. Phytopathology 89:197–203
- Donaldson L, Ludidi N, Knight MR, Gehring C, Denby K (2004) Salt and osmotic stress cause rapid increases in *Arabidopsis thaliana* cGMP levels. FEBS Lett 569:317–320
- Dubouzet JG, Sakuma Y, Ito Y, Dubouzet E, Miura S, Seki M, Shinozaki K, Yamaguchi-Shinozaki K (2003) OsDREB genes in rice, *Oryza sativa* L., encode transcription activators that function in drought-, high-, salt- and cold-responsive gene expression. Plant J 33:751–763
- Essah PA, Davenport R, Tester M (2003) Sodium influx and accumulation in *Arabidopsis*. Plant Physiol 133:307–318
- FAO (2011) FAO Land and Plant Nutrition Management Service. <http://www.fao.org/ag/agl/agl/spush>
- Felix G, Regenass M, Boller T (1993) Specific perception of subnanomolar concentrations of chitin fragments by tomato cells: induction of extracellular alkalization, changes in protein phosphorylation, and establishment of a refractory state. Plant J 4:307–316
- Felix G, Regenass M, Boller T (2000) Sensing of osmotic pressure changes in tomato cells. Plant Physiol 124:1169–1180
- Felle HH, Kondorosi E, Kondorosi A, Schultze M (1998) The role of ion fluxes in Nod factor signalling in *Medicago sativa*. Plant J 13:455–463
- Flescher E (2007) Jasmonates in cancer therapy. Cancer Lett 245:1–10
- Flowers T (2006) Preface. J Exp Bot 57:iv
- Fonseca S, Chico JM, Solano R (2009) The jasmonate pathway: the ligand, the receptor and the core signalling module. Curr Opin Plant Biol 12:539–547
- Gaff DF, Okong'O-Ogola O (1971) The use of non-permeating pigments for testing the survival of cells. J Exp Bot 22:756–758
- Gao XP, Pan QH, Li MJ, Zhang LY, Wang XF, Shen YY, Lu YF, Chen SW, Liang Z, Zhang DP (2004) Abscisic acid is involved in the water stress-induced betaine accumulation in pear leaves. Plant Cell Physiol 45:742–750
- Gaxiola RA, Rao R, Sherman A, Grisafi P, Alper SL, Fink GR (1999) The *Arabidopsis thaliana* proton transporters, AtNHX1 and Avp1, can function in cation detoxification in yeast. Proc Natl Acad Sci U S A 96:1480–1485
- Geilfuss CM, Mühling KH (2013) Ratiometric monitoring of transient apoplastic alkalizations in the leaf apoplast of living *Vicia faba* plants: chloride primes and PM-H⁺-ATPase shapes NaCl-induced systemic alkalizations. New Phytol 197:1117–1129
- Harper JF, Breton G, Harmon A (2004) Decoding Ca²⁺ signals through plant protein kinases. Annu Rev Plant Physiol Plant Mol Biol 55:263–288
- Hasegawa PM, Bressan RA, Zhu JK, Bohnert HJ (2000) Plant cellular and molecular responses to high salinity. Annu Rev Plant Physiol Plant Mol Biol 51:463–499
- Hong Y, Pan X, Welti R, Wang X (2008) Phospholipase Dα3 is involved in the hyperosmotic response in *Arabidopsis*. Plant Cell 20:803–816
- Hoson T (1998) Apoplast as the site of response to environmental signals. J Plant Res 111:167–177
- Huang GT, Ma SL, Bai LP, Zhang L, Ma H, Jia P, Liu J, Zhong M, Guo ZF (2012) Signal transduction during cold, salt, and drought stresses in plants. Mol Biol Rep 39:969–987
- Ingram J, Bartels D (1996) The molecular basis of dehydration tolerance in plants. Annu Rev Plant Physiol Plant Mol Biol 47:377–403
- Ippolito JA, Barbarick KA (2000) Modified nitric acid plant tissue digest method. Commun Soil Sci Plan 31:2473–2482
- Ishitani M, Xiong L, Stevenson B, Zhu JK (1997) Genetic analysis of osmotic and cold stress signal transduction in *Arabidopsis*: interactions and convergence of abscisic acid-dependent and abscisic acid-independent pathways. Plant Cell 9:1935–1949
- Ismail A, Riemann M, Nick P (2012) The jasmonate pathway mediates salt tolerance in grapevines. J Exp Bot 63:2127–2139
- Jabs T, Tschöpe M, Colling C, Hahlbrock K, Scheel D (1997) Elicitor stimulated ion fluxes and O₂⁻ from the oxidative burst are essential components in triggering defense gene activation and phytoalexin synthesis in parsley. Proc Natl Acad Sci U S A 94:4800–4805
- Jang M, Cai L, Udeani GO, Slowing KV, Thomas CF, Beecher CW, Fong HH, Farnsworth NR, Kinghorn AD, Mehta RG, Moon RC, Pezzuto JM (1997) Cancer chemopreventive activity of resveratrol, a natural product derived from grapes. Science 275:218–220
- Kenton P, Mur L, Atzorn R, Wasternack C, Draper J (1999) (-)-Jasmonic acid accumulation in tobacco hypersensitive response lesions. Mol Plant Microbe Interact 12:74–78
- Klobus G, Janicka-Russak M (2004) Modulation by cytosolic components of proton pump activities in plasma membrane and tonoplast from *Cucumis sativus* roots during salt stress. Physiol Plant 121:84–92
- Knight H, Trewavas AJ, Knight MR (1997) Calcium signalling in *Arabidopsis thaliana* responding to drought and salinity. Plant J 12:1067–1078
- Krisa S, Larronde F, Budzinski H, Decendit A, Deffieux G, Mérillon JM (1999) Stilbene production by *Vitis vinifera* cell suspension cultures: methyl jasmonate induction and ¹³C biolabeling. J Nat Prod 62:1688–1690
- Kronzucker HJ, Britto DT (2011) Sodium transport in plants: a critical review. New Phytol 189:54–81
- Lehmann J, Atzorn R, Brückner C, Reinbothe S, Leopold J, Wasternack C, Parthier B (1995) Accumulation of jasmonate, abscisic acid, specific transcripts and proteins in osmotically stressed barley leaf segments. Planta 197:156–162
- Miller G, Suzuki N, Ciftci-Yilmaz S, Mittler R (2010) Reactive oxygen species homeostasis and signalling during drought and salinity stresses. Plant Cell Environ 33:453–467
- Monshausen GB, Bibikova TN, Weisenseel MH, Gilroy S (2009) Ca²⁺ regulates reactive oxygen species production and pH during mechanosensing in *Arabidopsis* roots. Plant Cell 21:2341–2356
- Moons A, Prinsen E, Bauw G, Van Montagu M (1997) Antagonistic effects of abscisic acid and jasmonates on salt stress-inducible transcripts in rice roots. Plant Cell 9:2243–2259
- Munns R, Tester M (2008) Mechanisms of salinity tolerance. Annu Rev Plant Biol 59:651–681

- Padan E, Venturi M, Gerchman Y, Dover N (2001) Na⁺/H⁺ antiporters. *Biochim Biophys Acta* 1505:144–157
- Pauwels L, Barbero GF, Geerinck J, Tillemans S, Grunewald W, Pérez AC, Chico JM, Bossche RV, Sewell J, Gil E, García-Casado G, Witters E, Inzé D, Long JA, De Jaeger G, Solano R, Goossens A (2010) NINJA connects the co-repressor TOPLESS to jasmonate signalling. *Nature* 464:788–791
- Pedranzani H, Racagni G, Alemano S, Miersch O, Ramírez I, Peña-Corte H, Taleisnik E, Machado-Domenech E, Abdala G (2003) Salt tolerant tomato plants show increased levels of jasmonic acid. *Plant Growth Regul* 41:149–158
- Petit AN, Baillieux F, Vaillant-Gaveau N, Jacquens L, Conreux A, Jeandet P, Clément C, Fontaine F (2009) Low responsiveness of grapevine flowers and berries at fruit set to UV-C irradiation. *J Exp Bot* 60:1155–1162
- Qiao F, Chang X, Nick P (2010) The cytoskeleton enhances gene expression in the response to the Harpin elicitor in grapevine. *J Exp Bot* 61:4021–4031
- Qiu QS, Guo Y, Dietrich MA, Schumaker KS, Zhu JK (2002) Regulation of SOS1, a plasma membrane Na⁺/H⁺ exchanger in *Arabidopsis thaliana*, by SOS2 and SOS3. *Proc Natl Acad Sci U S A* 99:8436–8441
- Qiu QS, Guo Y, Quintero FJ, Pardo JM, Schumaker KS, Zhu JK (2004) Regulation of vacuolar Na⁺/H⁺ exchange in *Arabidopsis thaliana* by the salt-overly-sensitive (SOS) pathway. *J Biol Chem* 279:207–215
- Repka V, Fischerová I, Šilhárová K (2004) Methyl jasmonate is a potent elicitor of multiple defense responses in grapevine leaves and cell-suspension cultures. *Biol Plant* 48:273–283
- SAS (2000) Statistical Analysis Software Version 2000. SAS, Raleigh
- Seibicke T (2002) Untersuchungen zur induzierten Resistenz an *Vitis* spec. Ph.D. thesis, University of Freiburg
- Seo JS, Joo J, Kim MJ, Kim YK, Nahm BH, Song SI, Cheong JJ, Lee JS, Kim JK, Choi YD (2011) OsBHLH148, a basic helix-loop-helix protein, interacts with OsJAZ proteins in a jasmonate signaling pathway leading to drought tolerance in rice. *Plant J* 65:907–921
- Shabala S, Newman I (2000) Salinity effects on the activity of plasma membrane H⁺ and Ca²⁺ transporters in bean leaf mesophyll: masking role of the cell wall. *Ann Bot* 85:681–686
- Shabala S, Demidchik V, Shabala L, Cuin TA, Smith SJ, Miller AJ, Davies JM, Newman IA (2006) Extracellular Ca²⁺ ameliorates NaCl-induced K⁺ loss from *Arabidopsis* root and leaf cells by controlling plasma membrane K⁺-permeable channels. *Plant Physiol* 141:1653–1665
- Shavrukov Y (2013) Salt stress or salt shock: which genes are we studying? *J Exp Bot* 64:119–127
- Staswick PE (2008) JAZing up jasmonate signaling. *Trends Plant Sci* 13:66–71
- Staswick PE, Tiryaki I (2004) The oxylipin signal jasmonic acid is activated by an enzyme that conjugates it to isoleucine in *Arabidopsis*. *Plant Cell* 16:2117–2127
- Suhita D, Raghavendra AS, Kwak JM, Vavasseur A (2004) Cytoplasmic alkalization precedes reactive oxygen species production during methyl jasmonate- and abscisic acid-induced stomatal closure. *Plant Physiol* 134:1536–1545
- Takeuchi K, Gyohda A, Tominaga M, Kawakatsu M, Hatakeyama A, Ishii N, Shimaya K, Nishimura T, Riemann M, Nick P, Hashimoto M, Komano T, Endo A, Okamoto T, Jikumaru Y, Kamiya Y, Terakawa T, Koshihara T (2011) RSOsPR10 expression in response to environmental stresses is regulated antagonistically by jasmonate/ethylene and salicylic acid signaling pathways in rice roots. *Plant Cell Physiol* 52:1686–1696
- Tassoni A, Fomalé S, Franceschetti M, Musiani F, Michael AJ, Perry B, Bagni N (2005) Jasmonates and Na-orthovanadate promote resveratrol production in *Vitis vinifera* cv. Barbera cell cultures. *New Phytol* 166:895–905
- Tester M, Davenport R (2003) Na⁺ tolerance and Na⁺ transport in higher plants. *Ann Bot* 91:503–527
- Thines B, Katsir L, Melotto M, Niu Y, Mandaokar A, Liu G, Nomura K, He SY, Howe GA, Browse J (2007) JAZ repressor proteins are targets of the SCFCO11 complex during jasmonate signalling. *Nature* 448:661–665
- Türkan I, Demiral T (2009) Recent developments in understanding salinity tolerance. *Environ Exp Bot* 67:2–9
- Wang W, Tang K, Yang HR, Wen PF, Zhang P, Wang HL, Huang WD (2010) Distribution of resveratrol and stilbene synthase in young grape plants (*Vitis vinifera* L. cv. Cabernet Sauvignon) and the effect of UV-C on its accumulation. *Plant Physiol Biochem* 48:142–152
- Wasternack C (2007) Jasmonates: an update on biosynthesis, signal transduction and action in plant stress response, growth and development. *Ann Bot* 100:681–697
- Wolf S, Hématy K, Höfte H (2012) Growth control and cell wall signaling in plants. *Annu Rev Plant Biol* 63:381–407
- Ye H, Du H, Tang N, Li X, Xiong L (2009) Identification and expression profiling analysis of TIFY family genes involved in stress and phytohormone responses in rice. *Plant Mol Biol* 71:291–305
- Yoshida Y, Kiyosue T, Katagiri T, Ueda H, Mizoguchi T, Yamaguchi-Shinozaki K, Wada K, Harada Y, Shinozaki K (1995) Correlation between the induction of a gene for Δ^1 -pyrroline-5-carboxylate synthetase and the accumulation of proline in *Arabidopsis thaliana* under osmotic stress. *Plant J* 7:751–760
- Yoshimoto K, Jikumaru Y, Kamiya Y, Kusano M, Consonni C, Panstruga R, Ohsumi Y, Shirasu K (2009) Autophagy negatively regulates cell death by controlling NPR1-dependent salicylic acid signaling during senescence and the innate immune response in *Arabidopsis*. *Plant Cell* 21:2914–2927
- Zhang L, Xing D (2008) Methyl jasmonate induces production of reactive oxygen species and alterations in mitochondrial dynamics that precede photosynthetic dysfunction and subsequent cell death. *Plant Cell Physiol* 49:1092–1111
- Zhu D, Cai H, Luo X, Bai X, Deyholos MK, Chen Q, Chen C, Ji W, Zhu Y (2012) Over-expression of a novel JAZ family gene from *Glycine soja*, increases salt and alkali stress tolerance. *Biochem Biophys Res Commun* 426:273–279
- Zhu JK (2002) Salt and drought stress signal transduction in plants. *Annu Rev Plant Biol* 53:247–273
- Zimmermann D, Reuss R, Westhoff M, Gessner P, Bauer W, Bamberg E, Bentrup FW, Zimmermann U (2008) A novel, non-invasive, online-monitoring, versatile and easy plant-based probe for measuring leaf water status. *J Exp Bot* 59:3157–3167